



V-LOAD ANALYSIS

An Approximate Procedure,
Simplified and Extended,
for Determining Moments and Shears
in Designing Horizontally-Curved
Open-Framed Highway Bridges

USS Highway Structures Design Handbook Chapter 12, Volume I

A Note of Caution

All data, specifications, suggested practices, and drawings presented herein, are based on the best available information and delineated in accordance with recognized professional engineering principles and practices, and are published for general information only. Procedures and products, suggested or discussed, should not be used without first securing competent advice respecting their suitability for any given application.

Publication of the material herein is not to be construed as a warranty on the part of United States Steel—or that of any person named herein—that these data and suggested practices are suitable for any general or particular use, or of freedom from infringement on any patent or patents. Further, any use of these data or suggested practices can only be made with the understanding that United States Steel makes no warranty of any kind respecting such use and the user assumes all liability arising therefrom.

CONTENTS

1. ABSTRACT	I/12.2		
2. INTRODUCTION	I/12.2		
3. V-LOAD THEORY	I/12.3		
Torsional Load	I/12.4		
Development of the V-Loads	I/12.4		
a. Calculation of V-Loads for a Two-Girder System	I/12.4		
b. Calculation of V-Loads for Multi-Girder Systems	I/12.5		
Effect of Torsion on Bending Moments —M/R ² Moment Correction	I/12.6		
4. FINITE-ELEMENT MODELS	I/12.7		
Description of the Bridge Schemes	I/12.7		
a. Cross-Section Description	I/12.7		
b. Girder Design	I/12.8		
Description of the Finite-Element Models	I/12.8		
5. LIVE-LOAD ANALYSIS	I/12.9		
MSC/NASTRAN Live-Load Analysis	I/12.9		
V-Load Live-Load Analysis	I/12.10		
6. BENDING MOMENTS FOR OPEN-FRAMED SYSTEMS	I/12.11		
Dead Load	I/12.11		
		a. Noncomposite	I/12.11
		b. Composite	I/12.12
		c. M/R ² Moment Correction	I/12.12
		Live Load	I/12.12
		Combined Dead and Live Load	I/12.13
		7. BENDING MOMENTS FOR CLOSED-FRAME SYSTEMS	I/12.13
		8. TORSIONAL STRESSES	I/12.14
		St. Venant Torsion	I/12.14
		Warping Torsion	I/12.14
		a. Calculation of Lateral Flange Warping Moments and Shears	I/12.15
		9. CONCLUSIONS	I/12.17
		10. SUMMARY	I/12.18
		11. APPENDIX A	I/12.19
		V-Load Example	I/12.19
		12. REFERENCES	I/12.24
		13. TABLES	I/12.25
		14. FIGURES	I/12.42

1. ABSTRACT

The V-Load method is an approximate procedure widely used for analyzing horizontally-curved open-framed highway bridges. In the past, this method was only proven valid for noncomposite open-framed bridges with foundations on a radial alignment; currently, however, such designs represent merely a small percentage of curved bridges now being planned. This report extends the method to include composite open-framed bridges with any general support configuration under normal highway loadings.

V-Load analysis results for noncomposite and composite bridges under dead load and live load were compared to corresponding results from the finite-element program MSC/NASTRAN. Three finite-element curved-bridge models, with different combinations of radial and skewed supports, were generated with MSC/NASTRAN. Percentage errors between V-Load and MSC/NASTRAN maximum dead-load moments were all less than 10 percent. However, the live-load V-Load results were strongly influenced by the lateral

distribution factors used to distribute the truck wheel loads to the individual girders. Distribution factors specified by the American Association of State Highway and Transportation Officials (AASHTO), gave generally acceptable V-Load results for the exterior girders, and very conservative results for the interior girders. The combined factored dead- and live-load V-Load results were considered acceptable for all preliminary designs, and for most final designs. In all cases, the composite slab and skewed supports had little or no effect on the accuracy of the V-Loads results.

Resistance to out-of-plane warping of the cross section is an important consideration for curved I-girders; therefore, approximate expressions are given to compute the warping stresses in the girder flanges. It is also shown that the V-Load method is not a valid approximation for closed-framed systems with horizontal lateral wind bracing near, or in, the plane of the bottom flanges. It is probable that closed-framed systems should be analyzed as equivalent boxes.

2. INTRODUCTION

Horizontally-curved composite I-girder bridges are being used increasingly for highway interchanges and river crossings. The principal reason for this is that highway planners operate under many constraints, and highway structures must often conform to a predetermined roadway alignment. Esthetically, curved-bridge girders are more pleasing than a series of straight girders along the chords of a roadway curve; they also offer several inherent advantages. Curved girders allow the use of longer spans, thereby eliminating much of the substructure. They also permit designers to take advantage of continuous composite construction which results in a stiffer structure, fewer expansion details, and greater vertical clearance because of shallower girders. Additionally, curved girder bridges are usually characterized by simpler and more uniform construc-

tion details, since girder spacing and the concrete slab overhang are ordinarily constant along the length of the structure.

There are, however, a few disadvantages to curved-bridge design. Curved-girder fabrication, shipping, and erection costs may be somewhat higher than those for straight girders; obviously, the savings gained from the given advantages should be weighed against these costs. Another problem has been the difficulty in mathematically analyzing curved girders; the behavior of a curved structure is far more complex than that of a straight one. For example, its curvature causes torsional loading on the girder; this complicates stress analysis. While rigorous computer methods are available for analyzing the forces in curved girders, bridge design engineers generally prefer simplified analysis

techniques that are more suitable for use in a design office.

In 1963, United States Steel published a Structural Report^{1*} that presented a simplified approximate analysis technique for open-framed curved I-girder bridges. Open framing was defined in this report as noncomposite I-girders connected by diaphragms (floor beams) or cross frames (K- or X-bracing) with no horizontal lateral bracing near, or in, the plane of the bottom flanges. For a continuous two-girder open-framed system, the bending moments and shears in the girders obtained by using the approximate method were compared with results obtained from a more complicated analysis using the principles of virtual work and consistent deformations. The agreement was excellent, but the approximate method as originally presented was too cumbersome and time consuming for actual design—particularly for multi-girder systems. Therefore, the method was modified and greatly simplified for multi-girder systems a couple of years later.² Agreement of the approximate moments and shears, with other more complicated analyses was, again, excellent.

Eventually, this approximate procedure became known as the V-Load method, because a large part of the torsional load on the girders is approximated by sets of vertical shears known as “V-Loads.” The V-Load method is now widely used in consulting engineering offices. According to a 1969 survey, the method was employed for the design of approximately 75 percent of curved-steel I-girder bridges in the United States.³

Formerly, the V-Load method had only been proven valid for noncomposite open-framed systems, with the bridge piers on radial alignment. In current practice, most curved bridges have a reinforced concrete slab and usually depend on composite action to resist the loads. Often, horizontal lateral bracing is unnecessarily included near, or in, the plane of the bottom flanges to

help resist wind loads, creating a so-called closed-frame system. Moreover, many curved bridge foundations are on skewed alignments because of roadway right-of-way requirements beneath the bridge or other geometric restrictions. Thus, to use the V-Load method with assurance, it must be shown that the results of the V-Load analysis are valid approximations for these common cases.

The study presented here extends the V-Load method to composite open-framed bridges (no horizontal lateral bracing) with any general support configuration by comparing the bending moments and shears resulting from the V-Load method to the results from several finite-element analyses. Noncomposite and composite bridges, with combinations of radial and skewed supports, were analyzed using both methods under AASHTO dead and live loadings. The effect of horizontal lateral bracing was also studied. Another important consideration in the design of curved I-girder bridges are the warping stresses (lateral bending stresses) that develop in the girder flanges. These stresses arise from resistance to the out-of-plane warping of a girder cross section that is caused by the torsional loads. The approximate calculation of these warping stresses is also presented.

Theoretical development of the V-Load method and calculation of V-Loads, are discussed first, followed by a description of the finite-element models. A comparison of all the resulting bending moments from the V-Load and finite-element methods are then shown for dead load, live load, and combined factored dead and live loads. This report concludes with a discussion of closed-framed systems and torsional warping stresses.

By generalizing the V-Load method to include almost any curved-bridge configuration, it becomes an even more valuable tool for bridge engineers, and should help increase the economic competitiveness of steel bridge designs.

*See REFERENCES

3. V-LOAD THEORY

Conceptually, the V-Load method is best considered as a two-step process. First, the curved structure is straightened out so that the applied vertical loads are assumed to induce only ordinary bending stresses. The objective of the second step is to apply additional fictitious forces to the straight structure so that the resulting internal forces are the same as those in the curved structure when it is subjected to vertical load only. To satisfy the requirements of static equilibrium, the applied fictitious forces must be determined so that they result in no net vertical, longitudinal, or transverse forces on the total structure. Thus, in the V-Load development, the curvature forces on the equivalent

straight structure are treated as self-equilibrating externally applied loads.

To illustrate this, consider the curved-bridge system shown in Figure 1a; this consists of two prismatic girders continuous over one interior support with full-depth cross-frames uniformly spaced at a distance “d” along Girder 1 (outside). Cross-frames provide the primary resistance to the torsional loads caused by the bridge curvature. In so doing, the cross-frames prevent the warping stresses from becoming too large by restricting the lateral bending of the girder flanges. Unlike their characterization as secondary members in straight bridges, the diaphragms or cross-frames in a

curved bridge must, therefore, be designed as primary load-carrying members.

In Figure 1a, Girder 1 has a radius of “R,” and the distance between the girders is “D.” In ordinary straight-bridge design, the girders would be isolated, then individually analyzed and designed. Since an equivalent straight structure is used in the V-Load method, the curved girders are also analyzed as isolated straight girders, using developed span lengths equal to their respective arc lengths, L_1 and L_2 .

TORSIONAL LOAD

The approximate calculation of the internal torsional load on each girder, caused by curvature, is illustrated in Figures 1b and 1c. Figure 1b is a plan view of the top flange of one of the girders. Assuming that the flanges resist the full moment, the longitudinal force in the flange at any point is equal to the vertical bending moment on a transverse section “M” in the girder at that point divided by the depth “h” between the centerlines of the top and bottom flanges. Because of the bridge curvature, these axial forces are not collinear along any given segment of the flange (Fig. 1c). Thus, to maintain equilibrium, radial forces must be developed. These distributed radial forces have a magnitude of M/hR . Their distribution follows the shape of the vertical bending moment diagram (Fig. 1b). Radial forces cause lateral bending of the girder flanges and this results in the development of warping stresses. Note that the radial component of the top flange forces is directed outward where the flange is in compression (positive bending), and inward where the flange is in tension (negative bending—over the interior support). The corresponding radial forces in the bottom flange are in the opposite direction. It is the moment of these equal opposing forces times the depth “h” that causes twisting of the girder about its longitudinal axis.

DEVELOPMENT OF THE V-LOADS

Figure 2a shows a segment of the curved top flange of the outside girder where it is in compression; the length is a distance $d/2$ on either side of a cross frame. (The lateral flange warping moments are not shown in the figure and are discussed later.) To determine the torsional load that is resisted internally at the cross frame, the assumption is made² that the distributed radial flange force has a constant intensity of M/hR over the segment, where “M” is the vertical bending moment in the curved girder at the cross frame. The force exerted on the flange by the cross frame is, therefore, equal to Md/hR . Equal and opposite reaction forces are developed in each flange of each curved girder in the system (H_1 and H_2 in Fig. 2b) at every cross frame. (It is assumed that no internal reactions are developed in the web.) In Figure 2b, H_1 and H_2 are shown acting on a free-body diagram of the cross frame at Section A-A of the example curved bridge; the equal opposing reaction forces are also shown acting on the girders. The forces at each end of the cross frame are counterclockwise torsional couples and the corresponding clockwise

couples acting on the girders essentially help prevent the girders from tipping over.*

To maintain equilibrium of the cross frame, vertical shear forces “V” must develop at each end of the cross frame as a result of cross-frame rigidity and end fixity. These shear forces then react on the girders, resulting in a set of self-equilibrating girder shears. It is clear, then, that these shears tend to increase the moments—caused by applied loads—on the outside girder. With all signs reversed, the same thing is true in regions of negative bending. The net effect is that the total load on the curved bridge is generally shifted toward the outside girder. These girder shears are applied as external loads to the equivalent straight structure so as to account for the curvature; these are known as the V-Loads. Applying the external V-Loads creates internal forces in the straight structure that will almost be the same as those that exist in the curved structure under applied vertical loads.

Thus, in a V-Load analysis of the above system, the vertical bending moments at the cross frames—in each of the isolated developed straight girders—caused by applied vertical loads, are first determined by applying these loads to the straight girders. These vertical bending moments will hereafter be referred to as primary moments and are designated M_{1p} in Girder 1, M_{2p} in Girder 2. The corresponding V-Load moments caused by the V-Loads— M_{1v} and M_{2v} —are then determined by applying the V-Loads, in the proper directions, to the straight girders at the cross frames. The final moments in the curved girders— M_1 and M_2 —are then obtained by simply summing the respective straight-girder primary and V-Load moments. The shears, reactions, and deflections in the curved girders are also determined in the same manner. First, however, a method is needed to calculate the V-Loads.

Calculation of V-Loads for a Two-Girder System

Calculation of the V-Loads for a two-girder system is illustrated with reference to Section A-A in Figure 2b.

Moment equilibrium gives

$$VD = (H_1 + H_2)h \quad (1)$$

The values of H_1 and H_2 shown in the figure are substituted in Equation 1 to obtain

$$V = \frac{M_1 + M_2}{(RD)/d} \quad (2)$$

or

$$V = \frac{M_1 + M_2}{K} \quad (3)$$

where K is equal to a constant, $(RD)/d$, which depends

*It is assumed that any remaining torsional moments between the cross frames are resisted internally by the girders through a combination of St. Venant and warping torsion.

only on the geometry of the curved-bridge system.* As noted, the final moments in the curved girders can be expressed by the following equations

$$M_1 = M_{1p} + M_{1v} \quad (4a)$$

$$M_2 = M_{2p} + M_{2v} \quad (4b)$$

The V-Load moments are assumed to be proportional to their respective girder lengths, thus

$$M_{2v} = -M_{1v} \left(\frac{L_2}{L_1} \right) \quad (5)$$

Substituting Equation 5 into Equation 4b, the sum of the final moments becomes

$$M_1 + M_2 = M_{1p} + M_{2p} + \left[M_{1v} \left(1 - \frac{L_2}{L_1} \right) \right] \quad (6)$$

Since M_{1v} is generally small compared to M_{1p} and M_{2p} , and the term $(1 - L_2/L_1)$ is also small, the last term in Equation 6 (in square brackets) is neglected. Therefore

$$M_1 + M_2 = M_{1p} + M_{2p} \quad (7)$$

Substituting Equation 7 into Equation 3 gives

$$V = \frac{M_{1p} + M_{2p}}{K} \quad (8)$$

Equation 8 stresses that the girder shears (the V-Loads on the straight structure) at the cross frames for a two-girder system are obtained with very good accuracy by simply summing the primary moments in the girders at each cross frame and dividing by K .

Calculation of V-Loads for Multi-Girder Systems

For a three-girder curved system, the cross-frame shears between the outside girder and center girder, and the shears between the center girder and inside girder are assumed to be equal. Thus, the V-Loads on the straight outside and inside girders are equal and opposite, and there are no V-Loads on the straight center girder since its cross-frame shears cancel.

For curved systems having more than three girders, the cross-frame shears are not equal. Therefore, the distribution of cross-frame shears across the section becomes important, and the relative stiffnesses of the adjacent girders must be considered. The problem becomes simpler if it is assumed that: 1) all girders in the section have almost the same vertical stiffness, 2) girder shears across the section are self-equilibrating, and 3) the loading on girders outside the longitudinal cen-

terline of the system is increased, while the loading on girders inside the longitudinal centerline is decreased.

An important assumption is then made regarding the apportionment of the cross-frame shears to the individual girders. This assumption considers the shear on a girder to be proportional to the distance of that girder from the longitudinal centerline of the bridge, which implies a linear distribution of girder shears across the section. It can then be visualized that a curved-bridge cross section, under a torsional moment induced by the curvature, rotates as a rigid body, shifting the load towards the outside girder. This image is assisted when the rigid concrete slab is added. Without this assumption, the V-Load method would not be practical for multi-girder systems, and it turns out that this is a reasonable approximation as long as all girders have almost the same vertical stiffness—a usual condition for curved bridges under normal highway loadings. However, in the case of curved bridges under exceptional conditions that result in girders with large stiffness variations, the girder-shear distribution may be non-linear and the method described above does not give a valid approximation of actual behavior. This is discussed later.

The calculation of the V-Loads for multi-girder systems, based on the above assumptions, can be illustrated with reference to the four-girder system shown in Figure 3a. The girders in the cross section are assumed to be equally spaced. It is also assumed that the section is in the positive moment region of a curved bridge and, as a result, is subjected to a net counterclockwise torque, from the internal radial forces “H” in each of the girder flanges. (These forces—not shown—are in the same direction as the forces in Figure 2b.) It is also assumed that the cross-frames are of sufficient rigidity so that torques in the individual girders at the section can be summed.

To equilibrate this net torque, internal cross-frame shears— V_1 , V_2 , and V_3 —are developed. These shears are shown acting at inflection points in the cross frames, which are assumed to be at distances a , b , and c from the respective girders (arbitrarily shown at the cross-frame mid-space in Figure 3a). Because these shears develop reactions at the adjacent girders, and the shears, V , on the outside and inside girders are assumed to be equal and opposite, $V = V_1 = V_3$. Invoking the assumption that the girder shears are proportional to the distance of the girders from the longitudinal centerline of the bridge, the magnitudes of the shears on the two interior girders are equal to $(1/3)V$. This also means that $V_2 = V_1 + (1/3)V = (4/3)V$. (The factor, $1/3$, is a proportionality factor based on the geometry of the bridge cross section.) Note that the girder shears add up to zero across the section as assumed. The V-Loads that would be applied to the straight structure, are shown below the section.

Next, moment equilibrium between the inflection points is enforced at the bottom of each girder and results in the following equations:

*The outside-girder radius R and cross-frame spacing d along the outside girder are always used for simplicity. In most cases, the ratio of radius to cross-frame spacing is constant, and the value of K does not change significantly.

$$V_1 a = H_1 h = \frac{M_1 d}{R} \quad (9a)$$

$$V_1 \left(\frac{D}{3} - a \right) + V_2 b = \frac{M_2 d}{R} \quad (9b)$$

$$V_2 \left(\frac{D}{3} - b \right) + V_3 c = \frac{M_3 d}{R} \quad (9c)$$

$$V_3 \left(\frac{D}{3} - c \right) = \frac{M_4 d}{R} \quad (9d)$$

where M_1 , M_2 , M_3 , and M_4 , are the final moments in the respective curved girders at the cross frames. Substituting $V_1 = V_3 = V$ and $V_2 = (4/3)V$, and solving the four equations simultaneously for V gives

$$V = \frac{M_1 + M_2 + M_3 + M_4}{\left(\frac{10 RD}{9d} \right)} \quad (10)$$

Note that the assumed distances to the inflection points have dropped out of the equations.

Relating the final girder moments to the primary bending moments as before results in:

$$M_1 + M_2 + M_3 + M_4 = M_{1p} + M_{2p} + M_{3p} + M_{4p} \quad (11)$$

Substituting this in Equation 10 gives

$$V = \frac{M_{1p} + M_{2p} + M_{3p} + M_{4p}}{\left(\frac{10 RD}{9d} \right)} \quad (12)$$

or the more general relationship

$$V = \frac{\Sigma M_p}{CK} \quad (13)$$

where ΣM_p is the summation of the primary moments in each girder at a particular cross frame, "C" is a coefficient which depends on the number of girders in the system, and "K" is equal to $(RD)/d$, as before. ("R," "D," and "d" are for the outside girder.) The following table lists the coefficient "C" for various multi-girder systems assuming equal girder spacing.

No. of Girders in System	Coefficient, C
2	1
3	1
4	10/9
5	5/4
6	7/5
7	14/9
8	12/7
9	15/8
10	165/81

Equation 13 is, therefore, the general equation for the V-Loads on the outside and inside girders of the equivalent straight structure at the cross frames for multi-

girder systems. The proper proportionality factors are applied to these values to obtain the V-Loads on the other equivalent straight girders in the section. Special attention must always be given to the direction of the loads.

EFFECT OF TORSION ON BENDING MOMENTS— M/R^2 MOMENT CORRECTION

In a curved girder, the bending and torsional moments are mathematically coupled; physically, this means that the bending moments are influenced by the torsional moments along a girder and vice versa. This is illustrated with reference to the infinitesimal segment of a curved girder shown in Figure 3b. The three equations of equilibrium for the segment are:

$$\Sigma F_z = 0, \frac{dV}{dx} + w = 0 \quad (14a)$$

$$\Sigma M_y = 0, \frac{dM}{dx} + \frac{T}{R} - V = 0 \quad (14b)$$

$$\Sigma M_x = 0, \frac{dT}{dx} - \frac{M}{R} + t = 0 \quad (14c)$$

where "w" is an externally-applied uniformly-distributed load, "t" is an externally-applied uniformly-distributed torque, and "V," "M," and "T" are the internal shear, bending moment, and torque, respectively, acting at a given cross section. Since "M" and "T" appear in both equations 14b and 14c, they are coupled and cannot be solved directly.

However, in most cases the central angle "θ" of the girder is small, or the radius is large so the T/R term in Equation 14b can be dropped. Certain simplifying approximations can then be made, as was done in deriving the V-Load method. For example, when T/R is nearly equal to zero, the bending moment caused by the applied loads can initially be evaluated by considering the curved girder to be straight (Equation 14b). Because "t" is usually zero, the approximate torsional moment per unit length, dT/dx , is then equal to M/R from Equation 14c, where "M" is approximately equal to the primary bending moment determined above. This distributed torque is a result of the aforementioned radial flange forces which were used to calculate the V-Loads. As noted, the V-Loads cause an additional bending moment that is then added to the primary bending moment.

For girders with very sharp radii or very large central angles, the T/R term may be significant, and the bending moments may be influenced by the torsional moments. Consequently, since the bending moments are used to calculate the V-Loads, more accurate bending moments are needed to account for the effect of torsion. In the V-Load method, an approximate adjustment can be made to the primary moments. Differentiating Equation 14b and substituting R_i , the radius of the girder under consideration for R gives:

$$\frac{d^2M}{dx^2} + \frac{1}{R_i} \left(\frac{dT}{dx} \right) - \frac{dV}{dx} = 0 \quad (15)$$

Substituting Equations 14a and 14c into Equation 15 gives:

$$\frac{d^2M}{dx^2} + \left(\frac{M}{R_i^2} - \frac{t}{R_i} \right) + w = 0 \quad (16)$$

Since d^2M/dx^2 and “w” in Equation 16 both represent distributed loads, the quantity $(M/R_i^2 - t/R_i)$ must also be a distributed load. This load may be applied to each of the developed straight girders as shown in Figure 4a (again assuming that “t” equals zero). (“M” here is the primary bending moment M_p .) Moments from the M/R_i^2 loads could then be added to the primary moments from the external loads to obtain more exact moments for calculating the V-Loads (Equation 13). However, because this M/R_i^2 moment correction is not

statically correct, it should only be used as an indicator to determine the accuracy of the V-Load assumptions. When M/R_i^2 moments become large, it indicates that the limits of validity of the V-Load assumptions are being reached.

Since the M/R_i^2 distributed load is not generally uniform, it may be difficult to apply this load to a girder to calculate the resulting moments. Therefore, an expression is given in Figure 4b for calculating approximate equivalent concentrated loads applied at grid points for an arbitrary distributed load.^{4*} The concentrated loads, P_{e1} , P_{e2} , etc. replace the non-uniform distributed load. Special attention must again be given to the direction of the loads: positive bending causes a downward load.

*See Fig. 2-45d, p. 120 in REFERENCE 4.

4. FINITE-ELEMENT MODELS

As previously noted, the finite-element method was used to check the accuracy of the V-Load method. Mathematical models of the preliminary designs of three curved I-girder bridges (including both noncomposite and composite), with full-depth cross frames and different combinations of radial and skewed supports, were developed. A special modeling technique was used so that cross-sectional warping of the girders could be included. A general description of the three bridge schemes is given below, followed by a brief description of the finite-element models.

DESCRIPTION OF THE BRIDGE SCHEMES

For this study, three curved-bridge schemes were selected, each of which was representative of a common highway structure concept. The layouts of the three bridges are similar except for the support configurations. Hereinafter, they will be referred to as:

Scheme A—radial supports

Scheme B—parallel skewed supports

Scheme C—two parallel skewed supports and one radial support

Plan views of the schemes (all noncomposite) are shown in Figures 5a, 5b, and 5c, respectively.

All three bridges are two-span continuous, nonprismatic, four-girder structures with unequal spans and compound radii. The location of the interior pier is indicated on the figure for each bridge. All schemes are initially open-framed, that is, with no horizontal lateral bracing. Generally, span lengths differ among the three schemes and are listed in the figure.

In each case, the left span is referred to as Span 1, and

the right span as Span 2. The radii, R_1 and R_2 , are the same for each scheme and are also listed. Cross-frame spacings along the outside girder are shown on each bridge. These spacings were selected for their effectiveness in minimizing lateral bending stresses in the flanges caused by warping of the girder cross sections. The cross frames are also numbered for future reference. Note that Schemes B and C have intersecting cross frames at the interior pier. The skew angle of the supports in Schemes B and C is approximately 41 degrees.

Cross-Section Description

All three bridge schemes have the same basic cross section (Fig. 6a). The section is 34 ft wide with a roadway width of 31 ft from curb to curb. The girders are all plate girders and are equally spaced at 8 ft, 10 inches. There is a 3-ft, 9-inch overhang on each side of the section. The section has a superelevation of 0.10 ft/ft, which was ignored in all subsequent calculations. The concrete slab is 8 inches thick with a 3.5-inch haunch over each girder (from the bottom of the slab to the top of the web). A slab thickness of 7.5 inches was input in all analyses, however, to allow for slab wear. The specified compressive strength of the concrete, f'_c , the modular ratio, n , and the rebar area, A_s , are also indicated in the figure.

A typical cross frame is shown in Figure 6b. The cross frames are K-braces made up of structural tees (WT5x13). The centroids of the horizontal tees are offset 4 inches from the top and bottom of the web. The web depth of all four girders in each scheme is 60 inches.

Girder Design

The preliminary designs of the girders were prepared with the girder-design program SIMON.⁵ Because SIMON is a straight-girder design program, certain adjustments were made to the program input so as to achieve an appropriate design. For example, dead and live loads on the girders had to be increased or decreased approximately 10 to 20 percent depending on whether they were outside or inside the longitudinal centerline of the system (to account for the effect of curvature or the V-Loads). Also, the yield stress of the flanges was reduced by 5 ksi to allow for the warping stresses. The girders were designed for noncomposite action under dead load and composite action under superimposed dead load and live loads using 50-ksi yield-strength steel and the Load Factor Design method in the American Association of State Highway and Transportation Officials (AASHTO) *Standard Specifications for Highway Bridges*.⁶ The girders were checked for fatigue under 500,000 cycles of truck loading and 100,000 cycles of lane loading.

Preliminary girder designs for Scheme A are shown in Figure 7. All girders are non-prismatic with thicker flanges over the interior pier. All webs are transversely stiffened. Girder designs for Scheme A are typical since the designs for Schemes B and C are very similar—the only difference being minor variations in flange thicknesses.

The resulting moments of inertia of the girders for all three schemes are listed in Table 1. In the SIMON designs for dead load on the non-composite structure (designated DL1, consisting of the weight of the girders and cross frames plus the wet concrete slab), the moment of inertia of the girder alone was used throughout. For the superimposed dead load on the composite structure (designated DL2, and consisting of parapets, railings, and wearing surface) and live load, composite moments of inertia for the girder, slab, and rebars were used in regions of positive bending. The long-term composite moment of inertia, calculated with the transformed 3n concrete section to account for the effects of creep, was used for superimposed dead load, and the short-term composite moment of inertia based on the transformed n concrete section was used for live load. In regions of negative bending (over the pier), the composite moment of inertia of only the girder and rebars was used; the concrete was assumed to be ineffective. (It has been shown that the girder and rebars are both effective over the interior support of composite girders.⁷)

DESCRIPTION OF THE FINITE-ELEMENT MODELS

Computer models of each of the three curved-bridge schemes were developed using the finite-element program MSC/NASTRAN.⁸ Noncomposite models were generated for all three schemes. Composite models, including concrete slab elements, were generated for

Schemes A and C only. The entire bridge was modeled in each case because the live loads were unsymmetrical. Appropriate boundary conditions were specified at all supports. The bridges were modeled as supported vertically and radially at all three supports, and supported longitudinally only at the interior support.

The MSC/NASTRAN BEAM element provides an extra degree of freedom to account for warping and allows the user to input the warping stiffness of the girder. However, using a series of single BEAM elements for each girder would not allow for the modeling of the full-depth cross frames, because the model would be only two-dimensional. Therefore, a modeling technique was used whereby the two flanges and web are modeled as separate BEAM elements.⁹ The individual bending stiffnesses of each of the three rectangular elements were input (individual warping stiffnesses were not input). The flange elements were then offset at each grid point to the appropriate location relative to the web elements as illustrated for Girder 1 on the perspective view of the noncomposite Scheme A model in Figure 8a. Figures 8b and 9a show the noncomposite models for Scheme B and C, respectively.

Next, all displacements and rotations at the flange grid points, except the rotation about the (vertical) Z-axis, were coupled to those of the web grid points through multipoint constraint equations so the three elements behaved as one I-girder. By leaving the rotation about the Z-axis uncoupled, an extra degree of freedom was created; the flanges were allowed to warp independently out-of-plane and develop warping stresses. (It is assumed that the out-of-plane warping of the web is negligible.) It also allowed the full-depth cross frames to be modeled, as shown, since the model is now three-dimensional. The cross frames were modeled with BEAM elements, with the horizontal elements offset 4 inches from the top and bottom of the web elements. The cross-frame members were modeled as structural tees, since MSC/NASTRAN allows the user to offset the shear center from the neutral axis. Two groups of three straight flange and web BEAM elements approximating the arc length of the curve were used for each girder between cross frames to approximate the curved girders.

Figure 9b shows the composite model for Scheme A. In the composite models, QUAD4 plate elements with bending stiffness through the thickness were used to model the concrete slab. The flange and web BEAM elements were offset the proper distances from the slab-element grid points, so each girder actually behaved compositely. A reduced equivalent thickness of concrete, based on the transformed rebar area, was input to the QUAD4 elements over the interior pier. This equivalent thickness was used to approximate the fact that only the girder and rebars are effective over the pier. For superimposed dead load, the elastic modulus of the concrete elements was reduced by two-thirds (equivalent to 3n concrete) to account for creep. A Poisson's ratio of 0.15 was assumed for the concrete.

A curved-bridge layout very similar to Scheme C has been studied using a curved-girder analysis program CUGAR 2.¹⁰ Therefore, as a check on the models, the MSC/NASTRAN bending moments for Scheme C were compared to those from CUGAR 2. The original cross

sections, cross-frame spacings, and loads given in Reference 10 were used. The agreement was excellent for both noncomposite and composite dead load moments (live-load moment comparisons were not made).

5. LIVE-LOAD ANALYSIS

Live-load analysis of a bridge is difficult because it involves moving loads. Live loads must be moved longitudinally along the bridge as well as laterally within their design lanes. There are several existing techniques that are used to determine bending moments and shears. In a live-load analysis of the entire bridge, unit loads can be moved across the bridge so that influence surfaces for selected points in the bridge can be developed. Moment and shear envelopes for the individual girders can then be determined by placing the truck loads near the maximum and minimum ordinates of the respective influence surfaces for specified girder locations. The envelopes give maximum live-load moments and shears for girder design, and maximum live-load moment and shear ranges for fatigue and shear-connector design. For a straight bridge, a simpler approach can be used to develop moment and shear envelopes from influence lines for the isolated girders. Live-load distribution factors, such as those specified by AASHTO, must then be used to distribute the wheel loads laterally to the individual girders. Rather than develop influence surfaces, this latter approach is also used for curved-bridge analysis with the V-Load method because the girders are analyzed as isolated straight girders. In either case, however, a computer program is desirable for developing the envelopes.

For this particular study, it is not practical to develop and compare the full moment envelopes in the girders calculated from influence surfaces in the curved bridge (using MSC/NASTRAN) and influence lines in the developed straight girders (using the V-Load method). Therefore, only three of the live-load bending moments are investigated: the negative moment at the pier, and positive moments at points near the maximum moment location in each span. Influence lines, generated by program SIMON for each girder, are used to determine the approximate position and direction of the loads for the minimum (negative) moment at the pier and the maximum (positive) moment in each span. SIMON usually considers both the AASHTO truck loading and lane loading in determining the moments from the influence lines. However, SIMON revealed that lane loading does not govern for any of the girders in these bridge schemes; therefore, it was not considered further. Since the influence surfaces for the curved bridges are not readily available, it is initially assumed

that the three loading positions are the same for the curved-bridge and straight-girder models.

MSC/NASTRAN LIVE-LOAD ANALYSIS

The MSC/NASTRAN live-load analysis of the curved bridges for these loading positions will be discussed first. The V-Load live-load analysis procedure will then be outlined. This will allow a comparison of the MSC/NASTRAN and V-Load live-load moments for Schemes A and C. The composite curved MSC/NASTRAN models are loaded with AASHTO HS20 trucks at each of the three loading positions determined from SIMON. AASHTO specifies that the trucks can be moved anywhere within a 12-ft wide design lane, which can be spaced anywhere from curb to curb across the roadway width. No fractional parts of design lanes can be used, and only one truck per lane is allowed. Since the roadway width for these bridges is 31 ft, only two design lanes (and corresponding HS20 trucks) are allowed on the bridge.

The HS20 truck has three axles, with the wheels spaced 6 ft apart laterally. The spacing between the front and middle axles is fixed at 14 ft. The spacing between the rear and middle axles is permitted to vary between 14 ft and 30 ft. A disadvantage of MSC/NASTRAN is that concentrated wheel loads must be applied at the grid points for QUAD4 elements. Since the grid-point spacing often does not correspond to the wheel and axle spacings given above, equivalent grid-point wheel loads had to be computed in both the longitudinal and lateral directions.

Figure 10a illustrates the calculation of the longitudinal equivalent grid-point wheel loads for Girder 4 of Scheme C. The tractor and trailer wheel loads, P_1 and P_2 , of one truck are shown.* The middle wheel of the truck is placed at the approximate location for maximum moment in Span 1 (at 0.4L). The direction of the truck is determined from the ordinates of the straight-girder influence line. The minimum rear-axle spacing of 14 ft is assumed to govern. The longitudinal grid-point loads shown are statically equivalent to the wheel loads.

*The two trucks are placed side-by-side at the same relative position on the bridge, so the longitudinal equivalent loads for all of the other wheels are assumed to be the same.

Figure 10b illustrates the calculation of lateral equivalent grid-point wheel loads for Girder 4 of Scheme C. The cross section shown is at grid-point line A, adjacent to the front wheels, P_1 . The longitudinal equivalent grid-point loads for the front wheels of the two trucks at grid-point line A are also shown. According to AASHTO, the trucks are assumed to occupy a width of 10 ft (including two ft of clearance on each side); therefore, the adjacent wheels of two trucks can be no closer to each other than 4 ft. Also, a wheel must be at least 2 ft from the base of any curb. When two lanes are loaded, no reduction in the wheel loads is allowed. Applying these rules, the equivalent longitudinal wheel loads are shifted radially inward in their design lanes to produce the maximum load on Girder 4. The equivalent lateral grid-point loads are then obtained by summing the statically equivalent wheel-load reactions. These grid-point loads are then applied to the MSC/NASTRAN model.*

Fig. 11 illustrates this further on a plot of the finite-element model for Scheme C; only the slab elements are plotted for clarity. The top left of the figure shows the approximate loading position and direction of the two trucks for maximum moment in Span 1 of Girder 4. Immediately to the right, is a plot which should show the 42 required equivalent grid-point loads for this loading, with the length of each load vector in the figure corresponding to the load magnitude (but the small loads are not visible). Similar plots are shown for the approximate loading position for maximum moment in Span 2 of Girder 4 at the bottom of the figure. The same procedure is used for all three loading positions on each girder. The trucks are shifted laterally to put the maximum wheel load over the particular girder being investigated.

V-LOAD LIVE-LOAD ANALYSIS

MSC/NASTRAN was also used for the V-Load analyses. For live load, composite developed straight models were generated with MSC/NASTRAN to determine the primary and V-Load moments. The effective width of the slab, as defined by AASHTO, was used in the models. Again, since the grid-point spacing does not agree with the axle spacing, equivalent longitudinal grid-point loads are used (including impact and live-load load factor). Equivalent lateral grid-point loads are not used because the models represent isolated girders. Instead, straight-girder live-load lateral distribution factors—defined by AASHTO as the fraction of a truck wheel load carried by a particular girder—are used to distribute the wheel loads laterally to the individual girders. Applying the AASHTO rules for the calculation, the values of these distribution factors for the girders in Schemes A and C are:

Exterior Girders 1 and 4: 1.423 wheels

Interior Girders 2 and 3: 1.606 wheels

These factors are used to determine the original primary live-load moments in the developed straight girders, for each of the three loading positions, as noted earlier.

A separate lateral distribution factor is needed to compute the V-Load live-load moments. The AASHTO live-load distribution factor, for multiple girder bridges is based upon the truck loading being positioned so as to produce the maximum possible moment alternately in each girder. For a given position of the trucks, however, the V-Loads act concurrently on all the girders; therefore, using the AASHTO distribution factors to compute the V-Loads would result in too much total V-Load on the structure. Because the V-Loads act concurrently, the summation of V-Load distribution factors across the section should equal the number of wheels on the structure. Since the lateral placement of the wheels has very little effect on the sum of the primary moments across a section, a wheel-load lateral distribution factor for V-Loads can be simply computed as

$$(D.F.)_{V-Load} = \frac{2N_L}{N_G} \quad (17)$$

where N_L is the number of lanes loaded, and N_G is the number of girders in the section. The V-Load distribution factor in this study is equal to 1.0 wheel. There is only one V-Load distribution factor for all the girders in a particular bridge.

To compute the live-load V-Loads on a specific girder, for a truck at a specific location on that girder, the original primary moments, M_p , in all the girders are factored by the ratio of the V-Load distribution factor to the appropriate AASHTO distribution factor.* The summation of these reduced primary moments, M'_p , at each cross frame is then used in Equation 13 to calculate the V-Loads for that girder. (The proper proportionality factor is again used to compute the V-Loads for the interior girders.) This set of V-Loads is then applied only to the given straight girder at each cross-frame location to determine the V-Load live-load moments in that girder. These V-Load moments are added to the original primary moments, M_p , in that girder to give an approximate total live-load moment diagram (not an envelope) for that loading position. The maximum and minimum live-load moments in the girder for the truck in that position can then be determined from this moment diagram. This is the procedure that is used to determine the approximate maximum and minimum live-load moments for the trucks at the three specific loading positions.

To develop moment envelopes, this procedure must be repeated for the truck at selected loading positions

*The wheel loads, P_1 and P_2 , include the AASHTO live-load impact factor of the closest girder, and the Maximum Load live-load load factor equal to $1.3 (5/3) = 2.17$. No wheel-load lateral distribution factor is used.

*In determining the original primary moments in all the girders, the truck should be placed at the same relative position in the span of each girder, as the truck on the girder being considered.

along each girder. Whereas only one set of V-Loads is required for dead load, many sets of V-Loads are required here. Additional sets of V-Loads may be needed to compute live-load shears and shear envelopes, reactions, deflections, and uplift because the loads and distribution factors may be different. (A computer program is desirable.) For example, according to

AASHTO, live-load deflections may be computed assuming all girders deflect equally, using the summation of girder moments of inertia at a section (if the cross frames are adequate to distribute the loads). The same distribution factor (Equation 17) is then applied to the wheel loads to compute the primary and V-Load deflections.

6. BENDING MOMENTS FOR OPEN-FRAMED SYSTEMS

Finite element MSC/NASTRAN analyses for dead load on the noncomposite structure were done for all three open-framed schemes. Analyses for dead load and AASHTO live load on the composite structure were done for Schemes A and C only. All analyses were done using the preliminary girder designs. The bending moments in each girder were compared with the bending moments from the corresponding V-Load analyses. The dead-load V-Load analyses were also done using MSC/NASTRAN straight-girder models.

A comparison of solutions by the two methods for dead-load moments on the noncomposite and composite structures are presented first and this is followed by a comparison of the live-load moments. Combined factored dead- and live-load moments are also presented for comparison.

DEAD LOAD

Noncomposite

The uniform dead load (DL1) for all the schemes is 1.210 k/ft on the outside and inside girders, and 1.227 k/ft on the two interior girders. These loads include an assumed weight for the girders and cross frames.

A sample calculation of the V-Loads for DL1 at Cross Frame 6 in Span 1 of Scheme A is presented in Table II (the cross-frame numbers are taken from Figure 5). The primary moments were determined by applying the dead load to the noncomposite straight-girder models. The V-Loads were then calculated using Equation 13, as shown (a minus sign indicates a downward-acting V-Load). Also shown at the bottom of Table II are the calculated V-Loads in the straight girders at other selected cross frames (all values have been rounded off). Note the change in sign of the V-Loads across the section at the pier as the girders go from positive to negative bending. These calculated V-Loads across the section are plotted in Figure 12. The girder shears in the corresponding curved MSC/NASTRAN model—as computed from the cross-frame shears—are also plotted for comparison. Within the spans (Cross Frames 6, 7, 14, and 15), the agreement is excellent. The assumption of a linear distribution of girder shears across the

section appears to be valid. At the pier (Cross Frame 11), the agreement is not as good, but the V-Loads here go directly into the support and contribute only to the reactions. Note that the girder shears are actually equal to zero at the end supports (Cross Frames 1 and 18). It is interesting to note, too, that the shears in the girders at each cross-frame section actually did add up to zero in the MSC/NASTRAN model. There is apparently no longitudinal distribution of the girder shears in the bridge (that develop due to curvature), which agrees with earlier assumptions.

Comparison of the maximum and minimum DL1 bending moments from MSC/NASTRAN and the V-Load method, for the four girders of Scheme A, is summarized at the beginning of Table III. The magnitude and location of the maximum moments in each span are given, as are the minimum moments at the pier. The corresponding primary moments are also presented. The maximum percentage errors between the MSC/NASTRAN- and V-Load-analysis moments are 6.2 percent for the critical positive moment (in Span 2 of Girder 2), and 4.3 percent for the critical negative moment (Girder 3). Complete bending moment diagrams for all four girders are shown in Figure 13. There is close agreement between the MSC/NASTRAN and V-Load curves. The difference between the primary and MSC/NASTRAN or V-Load diagrams represents the effect of the curvature. This difference, referred to here as the curvature moment, is plotted for the girders of Scheme A in Figure 14. It should be noted that, as expected, the curvature moments in Girders 1 and 2 are approximately equal and opposite to the moments in Girders 4 and 3, respectively. The MSC/NASTRAN and V-Load curves appear to be further apart in Figure 14 because of the change in scale. (The curvature moments are an order of magnitude smaller than the total bending moments.)

Similar results are also given for Schemes B and C in Table III. For Scheme B, the maximum percentage errors are 7.4 percent for the critical positive moment (in Span 2 of Girder 1), and 3.3 percent for the critical negative moment (Girder 4). For Scheme C, the maximum percentage errors are 5.3 percent for the critical

positive moment (in Span 2 of Girder 4), and 7.0 percent for the critical negative moment (Girder 4). All of the V-Load-noncomposite results are, therefore, well within ten percent of the MSC/NASTRAN results. It is clear that the presence of skewed supports had very little effect on the accuracy of the V-Load results. Figures 15 and 16 show bending-moment diagrams for Schemes B and C. Because curvature-moment diagrams for Schemes B and C are quite similar to those of Scheme A, they are not shown.

As mentioned earlier, the girders should have almost the same vertical stiffness in order to make valid the primary assumption used in calculating the V-Loads: the assumption being that the shears in each girder are proportional to the distance of the girder from the longitudinal centerline of the bridge. The three curved-bridge schemes in this study were designed for normal highway loadings and thus, because of geometry, the girders in each scheme do have nearly the same vertical stiffness. This has been confirmed by the linear distribution of girder shears in the MSC/NASTRAN models, shown for Scheme A in Figure 12, and by the accuracy of the V-Load results for DL1 load. For very unusual loadings, such as an additional dead load (heavy pipe, etc.) along one side of the bridge or any other asymmetric load on the cross section, the girders may not have comparable vertical stiffness. In such circumstances, the girder-shear distribution across the section may not be linear.

To illustrate, the moment of inertia of the outside girder in Span 1 of Scheme C was made approximately 55 percent larger than the moment of inertia of the other three girders in that span.* Comparison of the MSC/NASTRAN and V-Load results for this case (for the noncomposite structure under DL1 load) is presented in graphic form in Figure 17. Figure 17a shows a plot of the V-Loads and MSC/NASTRAN girder shears across the section at Cross Frame 7 near the center of Span 1. The shear distribution in the MSC/NASTRAN model is non-linear, the outside girder having a much larger shear than the other girders because the primary moments are proportionately larger. This discrepancy naturally affects the accuracy of the V-Load-analysis results. The bending-moment diagram for the outside girder is shown in Figure 17b. The MSC/NASTRAN and V-Load curves differ significantly from each other, particularly in Span 1. The error in maximum moment in Span 1 between MSC/NASTRAN and the V-Load method is approximately 15.0 percent (with the V-Load moment being unconservative). The larger shear in the outside girder also affects the shears in the other girders, since the girder shears must still add up to zero across the section. Consequently, the percent error is approximately the same in the other girders in Span 1. Therefore, for abnormal loading cases, a more detailed analysis should be done.

*The cross sections, cross-frame spacings, and loads from the original CUGAR 2 analysis were used.

Composite

The uniform superimposed dead load (DL2) on all the composite girders for all the schemes is 0.411 k/ft. The comparison of the maximum and minimum bending moments from MSC/NASTRAN and the V-Load method for Schemes A and C is shown in Table IV. For Scheme A, the maximum percentage errors between the MSC/NASTRAN- and V-Load-analysis moments are 7.1 percent for the critical positive moment (in Span 2 of Girder 4), and 4.8 percent for the critical negative moment (Girder 3). For Scheme C, the maximum percentage errors are 5.5 percent for the critical positive moment (in Span 2 of Girder 1), and 8.3 percent for the critical negative moment (Girder 4). All V-Load results are again within ten percent of the MSC/NASTRAN results. The moment diagrams for dead load on the composite structure are similar to the previous diagrams for the dead load on the noncomposite structure and are not shown.

M/R² Moment Correction

The M/R² moment correction was included in the dead-load analysis of all the non-composite and composite girders. The M/R_i² loads, calculated from the primary moments, were applied to the straight-girder models using the equivalent concentrated grid-point loads, mentioned earlier (Figure 4b). The moments from these loads were then added to the primary moments and used to calculate corrected V-Loads.

The three bridges in the study have outside girder radii of 600 ft and 300 ft. The squares of these large numbers in the denominator make the M/R_i² loads and moments almost negligible. This indicates that the V-Load method should give accurate results for these bridges, as was in fact the case. To confirm this, the V-Load analyses were repeated using the corrected V-Loads. The moment correction made insignificant difference (less than 1 percent) in the V-Load-analyses results for these particular bridges.

LIVE LOAD

The comparison of the approximate live-load bending moments from MSC/NASTRAN and the V-Load method, for the four girders of Schemes A and C, is presented in Table V. All moments are factored moments and include impact. The magnitude and location of the approximate maximum (positive) moments in each span are given, as are the approximate minimum (negative) moments at the pier. The corresponding primary moments are also shown. The relative position(s) of the middle wheel of each truck (or trucks) in the span is shown directly below each moment value.

In all cases, the V-Load-analysis moments in the interior girders (Girders 2 and 3) vary broadly from 20 to 55 percent conservative compared to the MSC/NASTRAN moments. The V-Load analysis moments in the exterior girders (Girders 1 and 4) are, in most cases, within 15 percent of the MSC/NASTRAN values. (Similar results have been noted in a live-load lateral distribution study of straight I-girder bridges,¹¹

which also made use of finite-element techniques.¹² It was found that for bridges with full-depth cross frames, the AASHTO distribution factors tend to put too much load on the interior girders. The AASHTO factors for exterior girders give much better results.)

Therefore, in an ancillary study, the V-Load live-load analyses for Schemes A and C were repeated, using different wheel-load lateral distribution factors to compute the primary moments in the exterior and interior girders. These revised factors were simply calculated from the equilibrium of a straight-bridge cross section undergoing a rigid-body rotation. This rotation is due to the torsional moment on the section caused by the eccentric wheel loads (with respect to the longitudinal centerline of the bridge) as the trucks are shifted towards the outside girder. It was assumed in the calculation that the full-depth cross-frames are stiff enough so the bridge section behaves as a rigid body, and that the girders all have the same vertical stiffness. These recalculated distribution factors were:

Exterior Girders 1 and 4: 1.611 wheels
Interior Girders 2 and 3: 1.204 wheels

The percentage errors between the MSC/NASTRAN- and V-Load analysis moments for the interior girders, using these factors, were all reduced from the former range of 20 to 55 percent to well within 10 percent. The percentage errors for the majority of the moments in the exterior girders were increased slightly with most errors occurring on the conservative side. The former 20 percent un-conservative error in negative moment at the pier for Girder 1 of Scheme C was, however, reduced to approximately 10 percent. Note that the approximate loading position(s) of the truck(s) in the span for this particular moment are different for the curved-bridge (MSC/NASTRAN) and straight-girder (V-Load) models. In all probability, this is due to the skewed support at the pier, and may have contributed to the larger percentage error for this girder. This was also the case for Girder 2 of Scheme C. All other critical loading positions in the curved bridges correspond to those in the straight girders. Thus, the correct solution for the distribution of wheel-loads to the girders, for bridges with full-depth cross frames, would seem to lie between the AASHTO factors and these recalculated factors.

The V-Load moments were approximately the same in all the girders using both sets of factors, since the distribution factors for the V-Loads in either case must

always add up to the number of wheels on the structure. Because the major difference occurred in the primary moments, the V-Load method results for live load are only as good as the distribution factors that are used to calculate the primary moments. In most cases, using the present AASHTO distribution factors gave satisfactory results for the exterior girders and very conservative results for the interior girders. Improved lateral distribution factors have been derived for fatigue design,¹³ but more research is apparently needed on distribution factors for strength design—at least for bridges with full-depth cross frames.

COMBINED DEAD AND LIVE LOAD

Comparison of the combined factored dead- and live-load bending moments from MSC/NASTRAN and the V-Load method, for the four girders of Schemes A and C, is presented in Table VI. These combined moments would be used for the strength design of the girders in the AASHTO Load Factor Design method. The sum of the maximum and minimum dead-load moments in the non-composite and composite girders in each span and at the pier has been factored by 1.3. These moments were then added to the respective factored live-load moments from Table V. (The relative position of the live load in each span is again indicated in Table VI.)

All the percentage errors between the combined MSC/NASTRAN- and V-Load-analysis moments in the exterior girders are well within 10 percent (the worst error being 8.4 percent on the conservative side). The combined positive V-Load-analysis moments in the spans of the two interior girders are approximately 18 to 28 percent conservative compared to the respective MSC/NASTRAN moments. The percentage errors for the combined moments in the interior girders at the pier are all within 10 percent on the conservative side. This is because the dead-load pier moments are a larger percentage of the total pier moment for these particular bridges and, in general, the dead-load errors were much smaller than the live-load errors. The results would be better for longer-span bridges, where dead load is a still larger percentage of the total load. It should be emphasized that the bridge is always designed to be capable of resisting the total moment at any section; the moment is simply distributed to the girders in a slightly different way by the V-Load method. Thus, redistribution caused by V-Loads does not essentially change the overall bridge strength.

7. BENDING MOMENTS FOR CLOSED-FRAME SYSTEMS

Thus far, all the analyses were performed for open-framed systems, with no horizontal lateral bracing near, or in, the plane of the bottom flanges. Although bottom lateral wind bracing is not required for most I-girder bridges,¹⁴ it is sometimes included in some or all of the bays of sharply-curved I-girder bridges to help stabilize the girders during erection. It has been

shown that adding this bracing makes the girders behave like quasi-box girders; therefore, if lateral bracing is used, consideration should be given to a reduction in the lateral live-load distribution factor when computing moments and shears.¹⁵

To confirm this, lateral-bracing elements were added to the curved noncomposite and composite Scheme A

models in the plane of the bottom-flange elements. The bracing was selected to satisfy the maximum slenderness ratio, L/r , of 140 permitted by AASHTO for secondary members. Structural tees, WT6x32.5 with a cross-sectional area of 9.54 in.², were chosen. MSC/NASTRAN CONROD elements, with axial stiffness only, were used with lateral bracing in one case in every other bay (the two outside bays), and in the other case in all bays. The composite models with bracing in every other bay and in all bays are shown in Figure 18. The models are shown upside-down for clarity.

MSC/NASTRAN bending moments in all four girders are summarized in Table VII, for dead load on the noncomposite structure and super-imposed dead load on the composite structure, and for factored live load. The magnitude and location of the maximum moments in each span are given, as are the minimum moments at the pier. For live load, the relative positions of the middle wheels of the trucks in the span are again shown directly below each moment value. The moments for the bridge with lateral bracing, in every other bay and in all bays, are compared to the original moments for the bridge with no lateral bracing. For dead load, there was a definite redistribution of the load in all the girders when the bracing was added. In most cases, the moments in the girders were decreased, but some moments did increase slightly. For live load, there was a

significant decrease of the bending moments in almost all of the girders. For both dead and live load, there was little difference between the results of bracing all the bays compared to utilizing bracing in the outside bays only.

These results make obvious the fact that the bridge behaves as a different structure when the lateral bracing is added; the V-Load method assumptions are no longer valid. The composite bridge section, in particular, probably behaves more like a multi-cellular box girder, resisting the applied torque mainly through internal St. Venant shear flow. Equations are available to calculate an equivalent plate thickness for common configurations of truss-type lateral bracing.¹⁶ The section could then be analyzed as a multi-cellular box girder under combined bending and torsion. However, this analysis is likely to be more complicated than a V-Load analysis. Also, since the lateral bracing members become primary load-carrying members, they must be carefully designed to carry the loads, not simply selected for stiffness. The many additional connection details required for the bracing must also be carefully designed and fabricated to meet fatigue requirements. All of these factors must be weighed against the advantages that might be gained as a result of the improved load distribution (smaller girders, etc.).

8. TORSIONAL STRESSES

The V-Load method assumes that the internal torsional load on the bridge is resisted primarily by the shears that develop in the diaphragms or cross frames. Any remaining torque, however, must be resisted internally by the girders. An open section, such as an I-shaped girder, has two basic kinds of torsional resistance — St. Venant-stiffness and warping-torsional stiffness. Together, St. Venant and warping torsion cause additional bending stresses and shear stresses on the girder sections which must be accounted for. The warping stresses are particularly important for I-girders. The theory behind the development of these torsional stresses in open sections is well documented,^{17,18} and is summarized below. The approximate calculation of the warping stresses when using the V-Load method is also described. These stresses are then compared with the warping stresses computed from the curved MSC/NASTRAN models.

ST. VENANT TORSION

Pure St. Venant torsion in an I-girder is illustrated with reference to Figure 19a. The section shown is an unrestrained I-girder of constant cross section subjected to equal and opposite torques at the ends. As shown on the left, each element of the section twists through angle ϕ . It is assumed that the flanges and web

at any cross section retain their rectangular shapes during twisting. However, because the section is unrestrained and the shear deformations of the flanges and web are not uniform, the section will tend to warp out-of-plane as shown on the right.

The twisting of the section causes a shear flow, f_{sv} , to be set up inside the flanges and web in the direction of the resisting torque, T_{sv} . The St. Venant shear stress in each element of the section is equal to

$$\tau_{sv} = \frac{tT_{sv}}{K_{sv}} \quad (18)$$

where t is the thickness of the flanges or web, and K_{sv} is the St. Venant torsional stiffness of the entire section. This is the only stress associated with St. Venant torsion.

WARPING TORSION

Pure warping torsion in an I-girder would result when the out-of-plane warping of the section, mentioned above, is completely restrained (an ideal case). Warping-torsion stresses are caused by restraint of warping, not by warping. Restraint of warping is partly due to end support conditions; however, restraint of warping is also caused by a variation of torque along the span (as in a curved bridge).

The derivation of the warping torque and corresponding warping stresses is illustrated in Figure 19b. The figure on the left shows the girder section being twisted through angle Θ due to equal and opposite torques at each end. The flanges deflect laterally in opposite directions a distance u . Because the section is bending laterally and is now assumed to be restrained from warping out-of-plane, the self-equilibrating flange shear forces, V_{fw} , are developed. There is no net force on the section. These shear forces are in the direction of the resisting torque, T_w . The warping torque is therefore:

$$T_w = (V_{fw})h \quad (19)$$

where h is the vertical distance between the flange centerlines. It is again assumed that the elements of the section retain their shape during twisting, and that there is no lateral bending in the web. (This is a good assumption for most girders since the lateral bending stiffness of the web is usually negligible compared to that of the flanges.)

The flange shears cause lateral flange bending moments, M_{fw} , in the directions shown. It is these lateral flange shears and moments that cause warping shear stresses and warping normal bending stresses. The respective stress distributions are shown on the right of Figure 19b (note that the stresses are assumed to occur only in the flanges). For I-shaped girders only, these flange stresses may be easily computed from the shear- and flexural-stress equations for a rectangular section.* Assuming a parabolic shear stress distribution, the maximum warping shear stress at the junction of the flange and web is:

$$\tau_w = \frac{3V_{fw}}{2A_f} \quad (20)$$

where A_f is the cross-sectional area of the flange. This warping shear stress is generally small compared to the average shear stress in the web due to bending, and can often be neglected.

The maximum warping normal stress at the flange tip is:

$$\sigma_w = \frac{M_{fw}}{S_f} \quad (21)$$

where S_f is the section modulus of the rectangular flange about its strong axis. This stress may be significant and should not be ignored: it is usually on the order of 5 to 10 ksi. The maximum warping normal stress is combined with the maximum longitudinal bending stress (in the flange) to determine the maximum total flange stress.

Following this, to calculate the warping stresses, all that is needed are the lateral flange warping shears (V_{fw}) and bending moments (M_{fw}) in the curved girders. Practically, however, in most instances both

St. Venant torsion and warping torsion exist simultaneously. Curved-bridge girders are neither completely free to warp, nor is warping completely restrained. The degree of warping restraint varies along each span. Therefore, the St. Venant and warping torsion must also vary along the span. This is shown more clearly in Table VIII. The table lists the St. Venant and warping torques in Girder 1 of Scheme A for selected elements in each span of the noncomposite bridge. The values were determined from the curved MSC/NASTRAN model. Both the St. Venant and warping torques vary significantly along each span (note that they often oppose each other). More importantly, the warping torque is generally an order of magnitude larger than the St. Venant torque. (This is not surprising, since warping stiffness for I-shaped girders is much greater than the St. Venant stiffness.) Therefore, in the V-Load method the St. Venant torque — and its corresponding shear stresses — are neglected. It is assumed that all of the applied torque that is resisted internally by the girders is resisted in warping torsion only. This was also demonstrated in an earlier development of the V-Load method.¹

Calculation of Lateral Flange Warping Moments and Shears

In the V-Load method, each girder is isolated and analyzed as a developed straight girder to determine the vertical bending moments and shears. Similarly, to determine the lateral flange warping moments and shears in the V-Load method, each girder flange can be isolated and analyzed as a straight flange rigidly supported at every cross frame. Earlier, it was noted that for a curved bridge, the cross frames reduce lateral bending, and consequently, the warping stresses in the girder flanges. Thus, the cross frames act as lateral supports for the flanges. Lateral bending is caused by the radial flange forces due to curvature. Each straight flange model is, therefore, laterally loaded by the appropriate distributed radial flange force for that girder, $M/(hR)$, as shown in Figure 20. M is the total vertical bending moment in the girder, equal to the sum of the primary and V-Load moments.

Straight-flange models, for the top and bottom flanges of Girder 1 in Schemes A and C, were developed with MSC/NASTRAN. The $M/(hR)$ distributed loads, which follow the shape of the total vertical bending-moment diagram, were replaced with equivalent concentrated grid-point loads as illustrated previously in Figure 4b. The direction of the loads depended on whether the flange was in tension or compression. The lateral flange moment at each cross frame was then determined. (In all cases, the lateral flange moments at the cross frames were larger than the moments in-between the cross frames.) These moments were then compared to the corresponding moments from the MSC/NASTRAN curved-bridge models. In the curved-bridge models, the flanges were allowed to warp out-of-plane independently and develop the lat-

*For other shapes (tees, channels, and angles), the equations for a rectangular section are not valid. More complicated expressions must be used.

eral flange warping moments. Both flanges were modeled as separate elements, so the total lateral moment in each flange could simply be read off directly from the MSC/NASTRAN output. There was also a lateral moment in the flanges caused by a slight net radial movement of the entire bridge between supports. This radial rotation and deflection of the girder sections resulted in an additional lateral bending moment, M_{fb} , in each flange. Thus, the warping moment and the additional lateral bending moment had to be separated as parts of the total lateral moment.

The lateral flange warping and bending moments for Girder 1 of Scheme A are listed in Table IX. The top- and bottom-flange moments at all interior cross frames are shown. (The flange warping and bending moments at the end supports—Cross Frames 1 and 18—are zero.) Column 1 shows the flange warping moments, M_{fw} , derived from the computer output of the MSC/NASTRAN model for the noncomposite curved bridge. The corresponding flange warping moments derived from the straight-flange models are shown in Column 2. The agreement between the MSC/NASTRAN curved-bridge and straight-flange models is very good. Even though the top- and bottom-flange plates are not the same, the flange warping moments in the two flanges at each cross frame are generally equal and opposite. The flange warping moment depends mainly on the bridge geometry, in particular on the cross-frame spacing. The additional lateral flange bending moments, M_{fb} , at the cross frames from MSC/NASTRAN are shown in Column 3. These moments do depend on the stiffness of the flange, and are at least of an order of magnitude less than the flange warping moments. For this reason, they are ignored in the V-Load method. To confirm that the individual cross frames do act as almost rigid lateral flange supports, artificial rigid radial supports were added to all the girders in the MSC/NASTRAN curved-bridge model at each cross frame. Almost no change occurred in the flange warping moments; although, as expected, the lateral flange bending moments were reduced to even smaller values.

In both the curved-bridge and straight-flange models, there were only two flange elements between each pair of cross frames. While this is an acceptable mesh for longitudinal bending of each girder between supports, it is really too coarse for lateral bending of each flange between cross frames. Therefore, the straight-flange models were refined; each flange was modeled with four elements between adjacent cross frames. The results from these refined models are shown in Column 4 of Table IX. There was a significant change in the flange warping moments. These moments are considered more correct. However, the development of refined straight models for each flange of each girder is too tedious. A simpler approximation is needed for the V-Load method.

As before, a conservative assumption is made that the lateral distributed force on each flange has a constant value of $M/(hR)$, where M is the total vertical bending moment in the girder at each cross frame.

Since the cross frames are assumed to act as rigid supports for the flanges, the approximate flange warping moment at each cross frame can be calculated from the expression for the fixed-end moment in a straight beam under a uniformly distributed load.

$$M_{fw} = \frac{Md^2}{12hR} \quad (22)$$

Again, M is the total vertical bending moment (primary plus V-Load) in the girder at the cross frame. The noncomposite flange warping moments, calculated from this approximate formula, are listed in Column 5 of Table IX; they agree fairly well with the moments from the refined straight-flange models (Column 4) and are conservative in most cases.

The maximum warping normal stresses in each flange at the cross frames of the noncomposite bridge, calculated from Equation 21 using the approximate moments from Column 5, are shown in Column 6 (the maximum value in each flange is underlined). The sign of the stress at each flange tip depends on the direction of the flange warping moment. The flange warping shear at each cross frame can be approximated by

$$V_{fw} = \frac{\Delta M_{fw}}{d} \quad (23)$$

Where ΔM_{fw} is the difference in flange warping moments at adjacent cross frames. Equation 20 can then be used to calculate the maximum warping shear stress in the flanges, if desired.

The flange warping moments and warping normal stresses in Girder 1 of Scheme A—for dead load and live load on the composite bridge—are also shown in Columns 7 through 12 of Table IX. For live load, the moments and stresses for only two of the truck loading positions are shown.* The lateral warping moments were all calculated using the approximate expression (Equation 22).

In composite girders, the top flange and concrete slab act together to resist the top lateral warping moment. Though not calculated here, this warping moment has approximately the same magnitude as the corresponding moment in the bottom flange; however, the section modulus for lateral bending of the top flange and slab acting together is so large that the top warping stresses are negligible. Thus, only the warping moments and stresses in the bottom flange are shown. More detailed formulas are available to calculate the warping stresses in composite sections, if desired.¹⁹ These equations were used to check some of the composite DL2 and live-load warping moment and stress values in Table IX. The agreement was excellent. As expected, the warping normal stresses in the concrete slab and top flange were negligible, with the largest value being around 0.04 ksi.

*In actual design, envelopes should also be developed to determine the maximum and minimum live-load flange warping moments at each cross frame.

Finally, the flange warping moments and warping normal stresses in Girder 1 of Scheme C are shown in Table X. The warping moments were again calculated using the approximate Equation 22. Values are given for dead load on the noncomposite and composite

bridges, and for live load (for two truck loading positions). The largest warping normal stress found in Scheme A or C was 9.9 ksi. This stress could be reduced by increasing the lateral section modulus of the flange and/or decreasing the cross-frame spacing.

9. CONCLUSIONS

The V-Load method is a widely-used approximate method for analyzing horizontally-curved open-framed highway bridges. The procedure assumes that most of the internal torsional load on the bridge — resulting from the curvature — is resisted by self-equilibrating sets of diaphragm or cross-frame shears. These shears react on the individual girders and cause additional bending moments and shears in each girder. In general, the shears increase the moments due to applied loads on girders outside the longitudinal centerline of the bridge (away from the center of curvature) and decrease the moments due to applied loads on girders inside the longitudinal centerline. To account for this, these girder shears are applied as external loads (V-Loads) on an equivalent straight structure. The method conforms to conventional straight-bridge design, since the girders in the equivalent structure are isolated and analyzed as developed straight girders with span lengths equal to the curved-girder arc lengths.

Previously, the V-Load method had only been verified for noncomposite open-framed bridges (having no horizontal lateral bracing) with radially-aligned supports. In this study, the method was extended to composite open-framed bridges with more general support configuration. This was done by comparing the V-Load-analysis results to MSC/NASTRAN finite-element-analysis results for three preliminary curved-bridge schemes with various combinations of radial and skewed supports. Noncomposite and composite full-scale open-framed curved-bridge models, including full-depth cross frames, were developed with MSC/NASTRAN. The girders in each model all had warping degrees of freedom so the flanges could independently warp out-of-plane and develop lateral warping moments and warping normal stresses. These warping stresses are often significant in curved I-shaped-girder bridges.

The agreement between the V-Load and MSC/NASTRAN results (maximum and minimum girder bending moments) was excellent for dead load on the noncomposite and composite bridges. Corresponding moments from the two methods were within 10 percent of each other. The composite slab and skewed supports had no noticeable effect on the accuracy of the dead-load results. The accuracy of the V-Load live-load results, however, was strongly influenced by the lateral distribution factors that were used to determine the primary moments in each of the developed straight girders due to the design-truck wheel loads. The AASHTO distribution factors gave very conservative

V-Load live-load analysis results for the interior girders, and reasonably good results for the exterior girders. Different distribution factors, derived by assuming a rigid rotation of a straight-bridge cross section, gave greatly improved live-load results for the interior girders and generally more conservative results for the exterior girders. The skewed supports probably did have some minor effect on the live-load results, since the influence surfaces at a few locations on one of the skewed curved bridges apparently do not correspond to the respective influence lines in the developed straight girders.

The combined factored dead- and live-load V-Load-analysis moments, which would be used in actual girder design, agreed fairly well with the MSC/NASTRAN moments. The percentage errors in the exterior girders were all within 10 percent. The combined V-Load-analysis moments in the interior girders were all conservative to varying degrees, depending on the ratio of the dead- to live-load moments. The dead-load errors were usually less than the live-load errors; the worst dead-load error for all the schemes was 8.3 percent and the worst live-load error was 54.4 percent. For preliminary designs, and for most final designs, the combined-load results are acceptable—particularly for longer-span bridges where dead load predominates.

The warping stresses and flange warping moments, due to lateral bending of the girder flanges, were calculated with approximate formulas in the V-Load method. In this study, these stresses and moments agreed very well with the corresponding MSC/NASTRAN stresses and moments. For composite sections, the warping stresses in the top flanges and concrete slab are comparatively small and may be ignored. St. Venant torsional shear stresses in the girders also may be neglected.

The V-Load method can be used for curved girders having realistic radii, with limitations established by applying the optional M/R^2 moment correction. There are also some other limitations on the validity of the V-Load method. First, the method is only valid for loads such as normal highway loadings. For exceptional loadings, a more detailed analysis is required. The V-Load method assumes a linear distribution of girder shears across the bridge section. It was shown that the shear distribution becomes non-linear when the girders do not have approximately the same vertical stiffnesses at a given bridge cross section. This would be the case, for example, when there is an unusual asymmetric load on the bridge. It was shown that the V-Load-analysis

results differ significantly from the MSC/NASTRAN results for this case.

Secondly, the V-Load method is not directly applicable to a closed-framed system with horizontal lateral bracing near, or in, the plane of the bottom flanges. A bridge behaves differently when this bracing is added; the load distribution across the section is unlike that assumed by the V-Load method. The lateral bracing

members become primary load-carrying members. This was shown by adding lateral bracing elements to one of the curved-bridge models. Most of the bending moments in the girders were reduced significantly. Such a bridge should probably be analyzed as a multicellular box girder with the lateral bracing replaced by an equivalent plate.

10. SUMMARY

To summarize, the following general step-by-step procedure is presented for the V-Load analysis of any open-framed curved-bridge system under normal highway loadings.

- 1) Determine the primary moments due to the dead loads (DL1 and DL2) and live loads by applying those loads to the isolated developed straight girders (with span lengths equal to the curved-girder arc lengths). To determine live-load primary moments, use straight-girder lateral distribution factors to distribute the wheel or lane loads to the individual girders. Either the AASHTO factor or a more appropriate factor may be used.

OPTIONAL: For girders with very sharp radii, correct for the effect of torsion on the primary moments. Divide the primary moments by R_i^2 . Apply these M_p/R_i^2 distributed loads to the proper developed straight girders. Use the moments from the M_p/R_i^2 loads as an indicator to determine whether or not the limitations of the V-Load method are being reached.

- 2) From the summation of the primary moments in each girder at each diaphragm or cross frame, compute the V-Loads in the outside (largest radius) and inside (smallest radius) girders using Equation 13. To determine the V-Loads in the interior girders, factor these V-Loads by the correct proportionality factor. (The proportionality factor for the outside and inside girders is 1.0.) The V-Loads increase the loads on girders outside the longitudinal centerline and decrease the loads on girders inside the longitudinal centerline.

To compute the live-load V-Loads, first factor the primary moments by the ratio of the V-Load lateral distribution factor to the lateral distribution factor for the applied truck or lane loads. Then, use these reduced primary moments, M'_p , in Equation 13. The V-Load wheel-load lateral distribution factor is given by Equation 17.

- 3) Compute the V-Load moments by applying the V-Loads to the respective developed straight girders at each diaphragm or cross frame.

- 4) Add the V-Load moments to the primary moments from Step 1 to determine the final moments in the curved girders.

- 5) Compute the approximate flange warping moments at each diaphragm or cross frame using Equation 22. Then, compute the maximum warping normal stresses in the flanges from Equation 21. Superimpose the maximum warping normal stresses on the longitudinal bending stresses in the flanges. Approximate flange warping shears and warping shear stresses may also be computed from Equations 23 and 20, respectively.

- 6) Determine the shears, deflections, and reactions in the curved girders using the same procedure described above for moments.

For the live-load analysis, Steps 1 to 6 must be repeated for the truck or lane load at selected positions along each straight girder. Moment, shear, and flange warping-moment envelopes can then be developed. To calculate the V-Loads on a particular girder for the truck or lane load at a specific position on that girder, the truck or lane load must be placed at the same position in the span on each girder when computing the primary moments. Since different loads and distribution factors may be required to compute live-load shears, reactions, and deflections, different sets of these V-Loads may be needed.

In an actual bridge design, all of the above analysis steps would have to be repeated several times through the total design cycle as changes are made. Thus, the V-Load analysis really becomes too tedious for hand calculations. Therefore, the USS computer program V-LOAD is now available to do the total V-Load analysis for most practical curved I-girder bridge systems.²⁰ This program, developed for USS by Richardson, Gordon, and Associates, will reside on the USS CDC CYBER computer and will be available through USS Engineers and Consultants (UEC), a division of United States Steel Corporation, who maintain and market the USS library of programs.

11. APPENDIX A

V-LOAD EXAMPLE

The following example illustrates the analysis of a horizontally curved open-framed I-girder bridge (no horizontal lateral bracing) using the V-Load method. The previously described step-by-step procedure is employed. A plan view of this example: a four-girder, two-span continuous bridge (Scheme A) is shown in Figure 5. The bridge has all radial supports, unequal spans, and compound radii. The girder radii and span lengths, and cross-frame spacings along the outside girder are as indicated in the figure. The bridge cross section and a typical cross frame are shown in Figure 6. An elevation of the nonprismatic girder sections is given in Figure 7.

This example will illustrate the application of the V-Load method for noncomposite dead load (DL1) only. The dead load, DL1, on each of the girders is given at the top of Table II. For noncomposite dead load, the moments of inertia of the steel girders acting alone are used in the analysis. These moments of inertia along each span are listed for Scheme A at the top of Table I.

TABLE A
PRIMARY MOMENTS— M_p (K/ft)

CROSS-FRAME NUMBER	GIRDER 1	GIRDER 2	GIRDER 3	GIRDER 4
1	0.0	0.0	0.0	0.0
2	+487.7	+476.9	+458.0	+436.8
3	+916.9	+887.0	+842.3	+795.3
4	+1178.6	+1136.3	+1074.4	+1012.0
5	+1260.5	+1213.5	+1144.3	+1078.2
6	+1162.6	+1118.7	+1052.2	+994.2
7	+884.9	+851.8	+797.9	+759.8
8	+427.5	+412.9	+381.6	+375.1
9	-204.5	-193.7	-189.9	-153.7
10	-1014.6	-968.9	-924.8	-833.2
Pier 11	-1879.9	-1797.7	-1707.3	-1557.4
12	-1043.3	-995.4	-947.8	-854.7
13	-382.9	-360.8	-345.4	-296.8
14	+85.0	+89.0	+82.8	+99.0
15	+356.5	+351.5	+335.2	+332.3
16	+431.5	+424.9	+408.2	+398.0
17	+310.1	+305.3	+294.2	+285.2
18	0.0	0.0	0.0	0.0

The primary DL1 moment diagrams for each girder are shown in Figure 13.

STEP 1. Determine the Primary Moments M_p .

The first step in determining the primary moments is to isolate and straighten each girder. The developed span length of each straight girder is set equal to the respective curved-girder arc length. The primary moments are then determined by applying the proper load to each straight girder. Any readily available straight-girder analysis method may be used to determine these moments. (The results of such an analysis for each girder at each cross frame of the example bridge for DL1 are given in Table A; girder and cross-frame numbers relate to the numbers given in Figure 5, Scheme A.)

It should be observed that for a live-load V-Load analysis, straight-girder lateral distribution factors must be applied to the wheel or lane load before determining the primary moment.

OPTIONAL— M/R^2 Moment Correction

Since the radii of the girders in Span 1 (and a portion of Span 2) are fairly sharp, it should be determined if the torsion due to the curvature has any appreciable effect on the primary moments. The DL1 primary moments in each girder are divided by R_i^2 , where R_i is the radius of each girder, to give the following M_p/R_i^2 distributed loads (Table B).

TABLE B
 M_p/R_i^2 DISTRIBUTED LOAD (K/ft)

CROSS-FRAME NUMBER	GIRDER 1	GIRDER 2	GIRDER 3	GIRDER 4
1	0.0	0.00	0.0	0.0
2	+.0054	+.0056	+.0057	+.0058
3	+.0107	+.0105	+.0106	+.0106
4	+.0131	+.0134	+.0135	+.0135
5	+.0140	+.0143	+.0144	+.0144
6	+.0129	+.0132	+.0132	+.0133
7	+.0098	+.0100	+.0100	+.0102
8	+.0047	+.0049	+.0048	+.0050
9	-.0023	-.0023	-.0024	-.0021
10	-.0113	-.0114	-.0116	-.0111
Pier 11	-.0209	-.0212	-.0214	-.0208
12	-.0116	-.0117	-.0119	-.0114
13	-.0043	-.0043	-.0043	-.0040
14	+.0009	+.0011	+.0010	+.0013
15	+.0010	+.0010	+.0010	+.0010
16	+.0012	+.0012	+.0012	+.0012
17	+.0009	+.0009	+.0009	+.0009
18	0.0	0.0	0.0	0.0

TABLE C
 M_p/R_i^2 MOMENTS (K-ft)

CROSS-FRAME NUMBER	GIRDER 1	GIRDER 2	GIRDER 3	GIRDER 4
1	0.0	0.00	0.0	0.0
2	+4.4	+4.3	+4.1	+4.0
3	+8.8	+8.6	+8.2	+7.8
4	+11.9	+11.6	+10.9	+10.3
5	+13.1	+12.7	+12.0	+11.3
6	+12.3	+11.9	+11.1	+10.5
7	+9.6	+9.3	+8.6	+8.0
8	+5.5	+5.3	+4.8	+4.4
9	+0.7	+0.7	+0.4	+0.2
10	-3.7	-3.6	-3.7	-3.8
Pier 11	-8.3	-8.2	-8.1	-7.9
12	-7.4	-7.1	-7.0	-6.8
13	-6.4	-6.2	-6.1	-5.9
14	-4.9	-4.7	-4.6	-4.5
15	-3.3	-3.2	-3.2	-3.1
16	-2.1	-2.0	-2.0	-1.9
17	-1.0	-0.9	-0.9	-0.9
18	0.0	0.0	0.0	0.0

These distributed loads on each girder follow the shape of the primary moment diagrams as illustrated at the top of Figure 4. For convenience in determining the M_p/R_i^2 moments, these loads are used in the equation at the bottom of Figure 4 to determine equivalent concentrated loads at each cross frame. Each developed straight girder is then loaded with the appropriate set of equivalent concentrated loads to determine the following M_p/R_i^2 moments (Table C).

Because the M_p/R_i^2 moments are extremely small compared to the primary moments in each girder (less than 1%), it can be concluded that the effect of the torsion on the primary moments is negligible for this particular bridge. Consequently, the V-Load method can be expected to give accurate results.

STEP 2. Compute the V-Loads

The V-Loads on the outside (largest radius) and inside (smallest radius) girders at each cross frame are computed using Equation 13. The primary moments in the girders at each cross-frame section are summed and divided by the constant, CxK . The constant C is from the table on page I/12.6 and is equal to $10/9$ for a four-girder system (N.B. this table of constants is only valid for girders with equal lateral spacing. The constants must be rederived for unequal lateral spacings.) The constant K is based on the geometry of the curved-bridge system. A sample calculation of K for the girders in Span 1 of the example bridge (at Cross Frames 3 through 8) is shown at the top of Table II. In this example, K varies along the span since the diaphragm spacing d varies.

The V-Loads on the two interior girders are then computed by multiplying the V-Loads, calculated above, by the proper proportionality factor. This factor is based on the geometry of the bridge cross section. For the example bridge, the proportionality factor is equal to $\frac{1}{3}$ since the interior girders are one-third as far from the longitudinal centerline of the bridge as the exterior girders. This factor would also change with the number of girders in the curved-bridge section.

Special attention must always be given to the direction of the V-Loads. For girders outside the longitudinal centerline of the bridge, the V-Loads act downward (positive sign) in positive moment regions, and upward (negative sign) in negative moment regions. The opposite is true for girders inside the longitudinal centerline of the bridge. The computed DL1 V-Loads for the example bridge are listed below (Table D).

TABLE D
V-LOADS (kips)

CROSS-FRAME NUMBER	GIRDER 1	GIRDER 2	GIRDER 3	GIRDER 4
1	0.0	0.00	0.0	0.0
2	+2.57	+0.86	-0.86	-2.57
3	+4.76	+1.59	-1.59	-4.76
4	+6.09	+2.03	-2.03	-6.09
5	+6.50	+2.17	-2.17	-6.50
6	+6.00	+2.00	-2.00	-6.00
7	+4.56	+1.52	-1.52	-4.56
8	+2.21	+0.74	-0.74	-2.21
9	-1.03	-0.34	+0.34	+1.03
10	-4.59	-1.53	+1.53	+4.59
Pier 11	-9.00	-3.00	+3.00	+9.00
12	-5.54	-1.85	+1.85	+5.54
13	-2.00	-0.67	+0.67	+2.00
14	+0.51	+0.17	-0.17	-0.51
15	+0.99	+0.33	-0.33	-0.99
16	+1.20	+0.40	-0.40	-1.20
17	+0.86	+0.29	-0.29	-0.86
18	0.0	0.0	0.0	0.0

To compute live-load V-Loads, the live-load primary moments must first be factored by the ratio of the V-Load lateral distribution factor (Equation 17) to the straight-girder lateral distribution factor for the applied truck or lane load (used to calculate the primary moments). The reduced primary moments are then used in Equation 13.

STEP 3. Determine the V-Load Moments

The V-Load moments are computed by applying the above V-Loads to each of the respective developed straight girders at each cross frame. Again, any available straight-girder analysis method can be used. The results of such an analysis for the example bridge are given below for DL1 (Table E).

TABLE E
V-LOAD MOMENTS (K-ft)

CROSS-FRAME NUMBER	GIRDER 1	GIRDER 2	GIRDER 3	GIRDER 4
1	0.0	0.00	0.0	0.0
2	+167.5	+55.3	-54.5	-160.9
3	+337.5	+110.3	-107.4	-313.9
4	+455.2	+148.3	-143.7	-418.2
5	+500.0	+162.7	-157.2	-455.9
6	+467.0	+151.9	-146.1	-422.3
7	+362.4	+117.9	-112.5	-323.2
8	+203.5	+66.3	-61.9	-174.5
9	+20.3	+6.9	-4.0	-4.7
10	-151.6	-48.8	+50.9	+156.2
Pier 11	-265.6	-86.0	+87.5	+264.7
12	-286.3	-92.5	+93.2	+279.1
13	-242.8	-78.8	+79.6	+239.3
14	-176.4	-57.4	+58.3	+176.3
15	-143.7	-37.0	+38.0	+115.8
16	-62.5	-20.4	+21.1	+64.9
17	-26.2	-8.5	+8.9	+27.6
18	0.0	0.0	0.0	0.0

STEP 4. Determine the Final Moments in the Curved Girders

The final moments in the curved girders are then simply determined by adding the V-Load moments from Step 3 to the respective primary moments from Step 1. The final V-Load-analysis moments in the curved girders of the example bridge for DL1 are given in Table F.

TABLE F
FINAL V-LOAD ANALYSIS MOMENTS (K-ft)

CROSS-FRAME NUMBER	GIRDER 1	GIRDER 2	GIRDER 3	GIRDER 4
1	0.0	0.00	0.0	0.0
2	+655.2	+532.3	+403.5	+275.9
3	+1254.4	+997.3	+734.9	+481.4
4	+1633.8	+1284.6	+930.6	+593.7
5	+1760.5	+1376.2	+987.2	+622.3
6	+1629.6	+1270.6	+906.1	+571.9
7	+1247.3	+969.7	+685.4	+436.6
8	+630.9	+479.2	+319.6	+200.6
9	-184.2	-186.8	-193.9	-158.4
10	-1166.2	-1017.7	-873.9	-677.0
Pier 11	-2145.5	-1883.7	-1619.7	-1292.7
12	-1329.5	-1087.9	-854.5	-575.7
13	-625.7	-439.6	-265.8	-57.5
14	-91.4	+31.6	+141.1	+275.2
15	+243.2	+314.5	+373.1	+448.1
16	+369.0	+404.5	+429.3	+463.0
17	+284.0	+296.8	+303.2	+312.8
18	0.0	0.0	0.0	0.0

The V-Load analysis moment diagrams for each girder for DL1 are also shown in Figure 13.

STEP 5. Determine the Flange Warping Stresses

The warping stresses in the flanges of a curved I-girder bridge (due to lateral bending) are usually significant and should not be neglected. The first step in determining the flange warping normal stresses is to compute the flange warping moments at each of the cross frames using the approximate Equation 22. M in Equation 22 is the final moment in the curved girder at the cross frame (the moment computed in Step 4). The sign convention for the flange warping moment is shown at the top of Table IX. In positive bending regions, the flange warping moment is positive in the top flange and negative in the bottom flange for all girders in the section. The opposite is true in regions of negative bending. The approximate flange warping moments in the top and bottom flanges of Girder 1 in the example bridge at each cross frame for DL1 are given in column (5) of Table IX. (The moments at Cross Frames 1 and 18 are equal to zero.)

The next step is to determine the flange warping normal stresses from the flange warping moment using Equation 21. The computed DL1 warping normal stresses in the top and bottom flanges of Girder 1 in the example bridge at each cross frame are shown in column (6) of Table IX. (The stresses at cross-frames 1 and 18 are also equal to zero.) The sign of the stress at each flange tip depends on the direction of the flange warping moment. Similar computations should be repeated for each girder in the section using the appropriate values in Equations 21 and 22. The warping normal stresses should then be superimposed on the longitudinal bending stresses in the flanges (computed from the moments in step 4) to determine the total normal flange stress.

Approximate flange warping shears and warping shear stresses can also be computed from Equations 23 and 20, respectively, if desired. These stresses may or may not be significant, but should be checked.

STEP 6. Determine Shears, Deflections, and Reactions in the Curved Girders

Although not done here, the shears, deflections, and reactions in the curved girders can be computed in the same manner as illustrated in Steps 1 through 4. Primary shears, deflections, and reactions (from Step 1) are simply superimposed on V-Load shears, deflections, and reactions (from Step 3). For dead-load analyses, the same V-Loads that were computed in Step 2 to determine the bending moments in the curved girders can be used. For live-load analyses, however, different loads and lateral distribution factors may be required to determine the primary shears, deflections and reactions. Therefore, different sets of V-Loads may have to be computed in Step 2 for each case.

The above procedure (Steps 1 through 6) is the same for composite bridges and for bridges with skewed supports; simply use the appropriate span lengths and section properties. For superimposed dead load on the composite structure (DL2), the long-term composite moment of inertia—calculated with the transformed 3n concrete section—is used in positive bending regions. For live load, the short-term composite moment—calculated with the transformed n concrete section—is used in positive bending regions. In regions of negative bending, the composite moment of inertia of the girders and rebars alone was used for both DL2 and live load.*

One minor difference for composite bridges is that the warping stresses in the top flanges and concrete slab are very small and can usually be neglected. Also, it should be emphasized that in determining the moment, shear, and flange warping-moment envelopes in a live-load V-Load analysis, Steps 1 through 6 must be repeated for the truck or lane load at selected positions along each developed straight girder. To calculate the V-Loads on a particular girder for the truck or lane load at a specific position on that girder, the truck or lane load must be placed at the same position in the span on each girder in the section when computing the primary moment. Again, many sets of primary moments and corresponding V-Loads will be required. The USS V-LOAD computer program is recommended for a complete analysis.

*AASHTO Specifications (1985) will suggest use of the gross section in regions of negative bending.

12. REFERENCES

1. RICHARDSON, GORDON, AND ASSOCIATES, "Analysis and Design of Horizontally Curved Steel Bridge Girders," United States Steel Structural Report, ADUSS 88-6003-01, 1963.
2. "Highway Structures Design Handbook," Volume 1, Chapter 12, United States Steel Corporation, ADUSS 88-1895-01, 1965.
3. "Survey of Curved-Girder Bridges," by the Subcommittee on Curved Girders of the Joint AASHTO-ASCE Committee on Flexural Members, *Civil Engineering*, February 1973.
4. S.P. TIMOSHENKO, and J.M. GERE, *Theory of Elastic Stability*, McGraw-Hill Book Company, New York, 1961.
5. "SIMON—A Computer Program for the Design of Steel Girders," USS Engineers and Consultants, 600 Grant Street, Pittsburgh, PA.
6. *Standard Specifications for Highway Bridges*, The American Association of State Highway and Transportation Officials, 12th Edition, 1977.
7. P.S. CARSKADDAN, "Autostress Design of Highway Bridges Phase 3: Interior-Support-Model Test (AISI Project 188)," Research Report 97-H-045 (019-5), February 11, 1980.
8. C.W. MCCORMICK, Editor, "MSC/NASTRAN User's Manual," the MacNeal-Schwendler Corporation, Los Angeles, California 90041.
9. G. HAAIJER, Discussion of "Thin-Walled Curved-Beam Finite Element" by S.K. Chandhuri and S. Shore, *ASCE Engineering Mechanics Journal*, October 1978.
10. RICHARDSON, GORDON, AND ASSOCIATES, "Curved Girder Workshop," prepared for the Department of Transportation Federal Highway Administration, 1976.
11. "Live-Load Lateral Distribution for the Sunshine Skyway Approach Spans," USS Research Bulletin, April 2, 1982.
12. "Finite-Element Modeling Technique for Analysis of Live-Load Distribution in a Stringer Bridge," USS Research Bulletin, April 2, 1982.
13. C.G. SCHILLING, "Lateral Distribution Factors for Fatigue Design," *ASCE Structural Journal*, September 1982.
14. "Guide Specifications for Horizontally Curved Highway Bridges," The American Association of State Highway and Transportation Officials, 1980.
15. C.P. HEINS, AND J.O. JIN, "Load Distribution of Braced Curved I-Girder Bridges," University of Maryland, April 1982.
16. C.F. KOLBRUNNER, AND K. BASLER, "Torsion in Structures—An Engineering Approach," translated from the German, Springer-Verlag, New York, 1969.
17. C.G. SALMON, AND J.E. JOHNSON, *Steel Structures – Design and Behavior*, Harper & Row Publishers, New York, 1980.
18. W. MCGUIRE, *Steel Structures*, Prentice-Hall Inc., Englewood Cliffs, New Jersey, 1968.
19. C.P. HEINS, AND J.T.C. KUO, "Torsional Properties of Composite Girders," *AISC Engineering Journal*, Volume 9, No. 2, April 1972.
20. "V-LOAD — A Computer Program for the Analysis of Horizontally Curved Steel Bridge Girders," USS Engineers and Consultants, 600 Grant Street, Pittsburgh, PA.

13. TABLES

Table I
Moments of Inertia, inch⁴

I. Scheme A—Radial Supports

Positive Bending—Span 1			Negative Bending— Over Pier		Positive Bending—Span 2		
Girder	Girder + 3n Concrete	Girder + n Concrete	Girder	Girder + Rebars	Girder	Girder + 3n Concrete	Girder + n Concrete
1—38640	76704	109177	53949	63660	25138	52028	70974
2—34772	70102	98822	47133	56637	22932	51405	70878
3—30106	61444	85292	41268	50769	22179	49513	67929
4—24300	50094	68014	30807	40020	21565	45831	61943

II. Scheme B—Parallel Skewed Supports

Positive Bending—Span 1			Negative Bending— Over Pier		Positive Bending—Span 2		
Girder	Girder + 3n Concrete	Girder + n Concrete	Girder	Girder + Rebars	Girder	Girder + 3n Concrete	Girder + n Concrete
1—33447	66902	93538	49974	59694	23262	49806	67972
2—32154	66440	93436	47132	56637	24058	51720	70926
3—30106	61444	85292	43386	52426	23262	49806	67972
4—23087	51451	70886	35661	44549	20709	45616	61917

III. Scheme C—Two Parallel Skewed Supports and One Radial Support

Positive Bending—Span 1			Negative Bending— Over Pier		Positive Bending—Span 2		
Girder	Girder + 3n Concrete	Girder + n Concrete	Girder	Girder + Rebars	Girder	Girder + 3n Concrete	Girder + n Concrete
1—33447	66902	93538	53064	62570	24300	50094	68014
2—32154	66440	93436	47133	56637	24058	51720	70926
3—30106	61444	85292	41268	50769	21393	47572	64941
4—25943	53916	73895	31844	40788	19711	43533	58840

Table II

Calculation of V-Loads for DL1 (Noncomposite)

Scheme A—Radial Supports

Noncomposite 1.210 k/ft—Exterior Girders 1 and 4

Dead Load—DL1 = 1.227 k/ft—Interior Girders 2 and 3

Cross Frame 6—Span 1 $C = 10/9 = 1.1111$ Proportionality Factor = $1/3$

$$K = \frac{RD}{d} = \frac{(300)(26.5)}{12.222} = 650.5 \text{ ft.}$$

 M_{1p} = Primary moment in Girder 1 = +1162.6 k-ft M_{2p} = Primary moment in Girder 2 = +1118.7 k-ft M_{3p} = Primary moment in Girder 3 = +1052.2 k-ft M_{4p} = Primary moment in Girder 4 = +994.2 k-ft $\Sigma M_p = +4327.7 \text{ k-ft}$

$$\text{V-Load on Girder 1} = \frac{(4327.7)}{(1.1111)(650.5)} = -6.0 \text{ kips}$$

$$\text{V-Load on Girder 2} = 1/3(-6.0) = -2.0 \text{ kips}$$

$$\text{V-Load on Girder 3} = -1/3(-6.0) = +2.0 \text{ kips}$$

$$\text{V-Load on Girder 4} = -(-6.0) = +6.0 \text{ kips}$$

Cross Frame No.	V-Loads (kips)			
	Girder 1	Girder 2	Girder 3	Girder 4
1	0.0	0.0	0.0	0.0
6	-6.0	-2.0	+2.0	+6.0
7	-4.5	-1.5	+1.5	+4.5
Pier—11	+9.0	+3.0	-3.0	-9.0
14	-0.5	-0.2	+0.2	+0.5
15	-0.9	-0.3	+0.3	+0.9
18	0.0	0.0	0.0	0.0

Table III

Comparison of V-Load-Analysis Results with MSC/NASTRAN Results for DL1 (Noncomposite)

1.210 k/ft—Exterior Girders 1 and 4

1.227 k/ft—Interior Girders 2 and 3

I. Scheme A—Radial Supports**Girder 1 (Outside)**

Location	Primary Moment, k-ft (1)	MSC/NASTRAN Moment, k-ft (2)	V-Load-Analysis Moment, k-ft (3)	Percentage Error $100 \frac{(3)-(2)}{(2)}$
Maximum moment in Span 1 ($0.37L_1$)	+1262.9	+1731.6	+1760.8	+1.7
Minimum moment—pier	-1879.9	-2157.9	-2145.5	-0.6
Maximum moment in Span 2 ($0.75L_2$)	+425.4	+374.1	+373.7	-0.1

Girder 2

Location	Primary Moment, k-ft (1)	MSC/NASTRAN Moment, k-ft (2)	V-Load-Analysis Moment, k-ft (3)	Percentage Error $100 \frac{(3)-(2)}{(2)}$
Maximum moment in Span 1 ($0.37L_1$)	+1215.9	+1347.9	+1378.0	+2.2
Minimum moment—pier	-1797.7	-1947.4	-1883.7	-3.3
Maximum moment in Span 2 ($0.68L_2$)	+430.3	+382.8	+406.4	+6.2

Girder 3

Location	Primary Moment, k-ft (1)	MSC/NASTRAN Moment, k-ft (2)	V-Load-Analysis Moment, k-ft (3)	Percentage Error $100 \frac{(3)-(2)}{(2)}$
Maximum moment in Span 1 ($0.37L_1$)	+1147.1	+984.1	+990.4	+0.6
Minimum moment—pier	-1707.3	-1692.9	-1619.7	-4.3
Maximum moment in Span 2 ($0.67L_2$)	+412.9	+425.4	+434.7	+2.2

Girder 4 (Inside)

Location	Primary Moment, k-ft (1)	MSC/NASTRAN Moment, k-ft (2)	V-Load-Analysis Moment, k-ft (3)	Percentage Error $100 \frac{(3)-(2)}{(2)}$
Maximum moment in Span 1 ($0.37L_1$)	+1080.4	+625.0	+625.2	+0.03
Minimum moment—pier	-1557.4	-1313.7	-1292.7	-1.6
Maximum moment in Span 2 ($0.67L_2$)	+403.6	+461.9	+479.6	+3.8

II. Scheme B—Parallel Skewed Supports

Girder 1 (Outside)

Location	Primary Moment, k-ft (1)	MSC/NASTRAN Moment, k-ft (2)	V-Load-Analysis Moment, k-ft (3)	Percentage Error 100 $\frac{(3)-(2)}{(2)}$
Maximum moment in Span 1 (0.42L ₁)	+1012.2	+1396.7	+1432.6	+2.6
Minimum moment—pier	-1814.3	-2038.1	-1997.6	-2.0
Maximum moment in Span 2 (0.70L ₂)	+551.9	+520.8	+482.4	-7.4

Girder 2

Location	Primary Moment, k-ft (1)	MSC/NASTRAN Moment, k-ft (2)	V-Load-Analysis Moment, k-ft (3)	Percentage Error 100 $\frac{(3)-(2)}{(2)}$
Maximum moment in Span 1 (0.39L ₁)	+1058.2	+1212.2	+1191.0	-1.7
Minimum moment—pier	-1826.6	-1904.7	-1896.6	-0.4
Maximum moment in Span 2 (0.69L ₂)	+562.7	+542.3	+548.2	+1.1

Girder 3

Location	Primary Moment, k-ft (1)	MSC/NASTRAN Moment, k-ft (2)	V-Load-Analysis Moment, k-ft (3)	Percentage Error 100 $\frac{(3)-(2)}{(2)}$
Maximum moment in Span 1 (0.36L ₁)	+1077.7	+1013.9	+952.2	-6.1
Minimum moment—pier	-1822.3	-1756.0	-1751.9	-0.2
Maximum moment in Span 2 (0.68L ₂)	+563.9	+558.4	+570.0	+2.1

Girder 4 (Inside)

Location	Primary Moment, k-ft (1)	MSC/NASTRAN Moment, k-ft (2)	V-Load-Analysis Moment, k-ft (3)	Percentage Error 100 $\frac{(3)-(2)}{(2)}$
Maximum moment in Span 1 (0.39L ₁)	+1075.3	+684.8	+728.1	+6.3
Minimum moment—pier	-1822.9	-1573.7	-1625.1	+3.3
Maximum moment in Span 2 (0.67L ₂)	+547.8	+531.2	+549.0	+3.4

III. Scheme C—Two Parallel Skewed Supports and One Radial Support

Girder 1 (Outside)

Location	Primary Moment, k-ft (1)	MSC/NASTRAN Moment, k-ft (2)	V-Load-Analysis Moment, k-ft (3)	Percentage Error 100 $\frac{(3)-(2)}{(2)}$
Maximum moment in Span 1 ($0.36L_1$)	+975.1	+1393.1	+1392.6	-0.04
Minimum moment—pier	-1947.7	-2132.9	-2144.7	+0.6
Maximum moment in Span 2 ($0.71L_2$)	+672.6	+607.7	+617.8	+1.7

Girder 2

Location	Primary Moment, k-ft (1)	MSC/NASTRAN Moment, k-ft (2)	V-Load-Analysis Moment, k-ft (3)	Percentage Error 100 $\frac{(3)-(2)}{(2)}$
Maximum moment in Span 1 ($0.39L_1$)	+1060.8	+1205.6	+1196.9	-0.7
Minimum moment—pier	-1819.8	-1945.5	-1894.2	-2.6
Maximum moment in Span 2 ($0.69L_2$)	+552.9	+533.6	+536.8	+0.6

Girder 3

Location	Primary Moment, k-ft (1)	MSC/NASTRAN Moment, k-ft (2)	V-Load-Analysis Moment, k-ft (3)	Percentage Error 100 $\frac{(3)-(2)}{(2)}$
Maximum moment in Span 1 ($0.36L_1$)	+1120.0	+1007.2	+990.1	-1.7
Minimum moment—pier	-1706.6	-1687.0	-1633.4	-3.2
Maximum moment in Span 2 ($0.67L_2$)	+412.9	+415.9	+425.6	+2.3

Girder 4 (Inside)

Location	Primary Moment, k-ft (1)	MSC/NASTRAN Moment, k-ft (2)	V-Load-Analysis Moment, k-ft (3)	Percentage Error 100 $\frac{(3)-(2)}{(2)}$
Maximum moment in Span 1 ($0.44L_1$)	+1159.3	+770.5	+808.5	+4.9
Minimum moment—pier	-1571.3	-1287.9	-1378.6	+7.0
Maximum moment in Span 2 ($0.72L_2$)	+288.2	+319.6	+302.8	+5.3

Table IV

Comparison of V-Load-Analysis Results with MSC/NASTRAN Results for DL2 (Composite)

0.411 k/ft—All Girders

I. Scheme A—Radial Supports**Girder 1 (Outside)**

Location	Primary Moment, k-ft (1)	MSC/NASTRAN Moment, k-ft (2)	V-Load-Analysis Moment, k-ft (3)	Percentage Error $100 \frac{(3)-(2)}{(2)}$
Maximum moment in Span 1 ($0.42L_1$)	+470.7	+647.7	+670.2	+3.5
Minimum moment—pier	-550.4	-653.9	-654.6	+0.1
Maximum moment in Span 2 ($0.68L_2$)	+182.5	+164.8	+167.6	+1.7

Girder 2

Location	Primary Moment, k-ft (1)	MSC/NASTRAN Moment, k-ft (2)	V-Load-Analysis Moment, k-ft (3)	Percentage Error $100 \frac{(3)-(2)}{(2)}$
Maximum moment in Span 1 ($0.42L_1$)	+448.3	+499.3	+513.1	+2.8
Minimum moment—pier	-517.7	-567.1	-551.9	-2.7
Maximum moment in Span 2 ($0.68L_2$)	+177.9	+168.5	+173.0	+2.7

Girder 3

Location	Primary Moment, k-ft (1)	MSC/NASTRAN Moment, k-ft (2)	V-Load-Analysis Moment, k-ft (3)	Percentage Error $100 \frac{(3)-(2)}{(2)}$
Maximum moment in Span 1 ($0.42L_1$)	+423.4	+357.8	+360.5	+0.8
Minimum moment—pier	-494.0	-482.8	-459.7	-4.8
Maximum moment in Span 2 ($0.67L_2$)	+171.1	+172.8	+176.1	+1.9

Girder 4 (Inside)

Location	Primary Moment, k-ft (1)	MSC/NASTRAN Moment, k-ft (2)	V-Load-Analysis Moment, k-ft (3)	Percentage Error $100 \frac{(3)-(2)}{(2)}$
Maximum moment in Span 1 ($0.42L_1$)	+403.8	+219.7	+220.1	+0.2
Minimum moment—pier	-464.5	-366.0	-362.7	-0.9
Maximum moment in Span 2 ($0.67L_2$)	+168.1	+170.9	+183.0	+7.1

II. Scheme C—Two Parallel Skewed Supports and One Radial Support

Girder 1 (Outside)

Location	Primary Moment, k-ft (1)	MSC/NASTRAN Moment, k-ft (2)	V-Load-Analysis Moment, k-ft (3)	Percentage Error $100 \frac{(3)-(2)}{(2)}$
Maximum moment in Span 1 ($0.42L_1$)	+369.6	+520.5	+536.8	+3.1
Minimum moment—pier	-571.1	-641.0	-655.9	+2.3
Maximum moment in Span 2 ($0.65L_2$)	+271.2	+247.7	+261.4	+5.5

Girder 2

Location	Primary Moment, k-ft (1)	MSC/NASTRAN Moment, k-ft (2)	V-Load-Analysis Moment, k-ft (3)	Percentage Error $100 \frac{(3)-(2)}{(2)}$
Maximum moment in Span 1 ($0.39L_1$)	+397.0	+459.3	+451.9	-1.6
Minimum moment—pier	-520.1	-565.1	-549.7	-2.7
Maximum moment in Span 2 ($0.63L_2$)	+222.5	+220.9	+219.7	-0.5

Girder 3

Location	Primary Moment, k-ft (1)	MSC/NASTRAN Moment, k-ft (2)	V-Load-Analysis Moment, k-ft (3)	Percentage Error $100 \frac{(3)-(2)}{(2)}$
Maximum moment in Span 1 ($0.42L_1$)	+416.0	+362.8	+362.1	-0.20
Minimum moment—pier	-490.3	-478.7	-460.9	-3.7
Maximum moment in Span 2 ($0.67L_2$)	+172.1	+172.6	+173.1	+0.3

Girder 4 (Inside)

Location	Primary Moment, k-ft (1)	MSC/NASTRAN Moment, k-ft (2)	V-Load-Analysis Moment, k-ft (3)	Percentage Error $100 \frac{(3)-(2)}{(2)}$
Maximum moment in Span 1 ($0.44L_1$)	+436.9	+267.0	+282.6	+5.8
Minimum moment—pier	-459.5	-351.0	-380.0	+8.3
Maximum moment in Span 2 ($0.65L_2$)	+127.9	+129.8	+129.6	-0.2

Table V

Comparison of V-Load-Analysis Results with MSC/NASTRAN Results

Live Load—Two AASHTO HS20 Trucks— $1.3*[5/3(L+I)]$ **I. Scheme A—Radial Supports**

L = AASHTO HS20 Truck Wheel Load

I = AASHTO Impact Factor

Girder 1 (Outside)

Location	Primary Moment, k-ft (1)	MSC/NASTRAN Moment, k-ft (2)	V-Load-Analysis Moment, k-ft (3)	Percentage Error $100 \frac{(3)-(2)}{(2)}$
Positive moment in Span 1 (0.42L ₁)	+2681.1 (0.35L ₁)	+3648.0 (0.35L ₁)	+3562.6 (0.35L ₁)	-2.3
Negative moment—pier	-1032.9 (0.35L ₁)	-1525.4 (0.35L ₁)	-1335.3 (0.35L ₁)	-12.5
Positive moment in Span 2 (0.54L ₂)	+2035.5 (0.55L ₂)	+2541.6 (0.55L ₂)	+2400.0 (0.55L ₂)	-5.6

Girder 2

Location	Primary Moment, k-ft (1)	MSC/NASTRAN Moment, k-ft (2)	V-Load-Analysis Moment, k-ft (3)	Percentage Error $100 \frac{(3)-(2)}{(2)}$
Positive moment in Span 1 (0.42L ₁)	+2973.7 (0.35L ₁)	+2342.2 (0.35L ₁)	+3267.8 (0.35L ₁)	+39.5
Negative moment—pier	-1330.6 (0.54L ₁)	-1155.6 (0.54L ₁)	-1438.3 (0.54L ₁)	+24.5
Positive moment in Span 2 (0.53L ₂)	+2222.0 (0.55L ₂)	+1787.3 (0.55L ₂)	+2367.5 (0.55L ₂)	+32.5

Girder 3

Location	Primary Moment, k-ft (1)	MSC/NASTRAN Moment, k-ft (2)	V-Load-Analysis Moment, k-ft (3)	Percentage Error $100 \frac{(3)-(2)}{(2)}$
Positive moment in Span 1 (0.37L ₁)	+2906.9 (0.35L ₁)	+1895.2 (0.35L ₁)	+2627.4 (0.35L ₁)	+38.6
Negative moment—pier	-1358.6 (0.54L ₁)	-875.3 (0.54L ₁)	-1246.3 (0.54L ₁)	+42.4
Positive moment in Span 2 (0.53L ₂)	+2137.3 (0.55L ₂)	+1528.2 (0.55L ₂)	+2076.0 (0.55L ₂)	+35.8

Girder 4 (Inside)

Location	Primary Moment, k-ft (1)	MSC/NASTRAN Moment, k-ft (2)	V-Load-Analysis Moment, k-ft (3)	Percentage Error $100 \frac{(3)-(2)}{(2)}$
Positive moment in Span 1 (0.37L ₁)	+2525.4 (0.35L ₁)	+1914.5 (0.35L ₁)	+1711.2 (0.35L ₁)	-10.6
Negative moment—pier	-1213.8 (0.54L ₁)	-944.9 (0.54L ₁)	-866.6 (0.54L ₁)	-8.3
Positive moment in Span 2 (0.53L ₂)	+1833.0 (0.55L ₂)	+1680.7 (0.55L ₂)	+1572.6 (0.55L ₂)	-6.4

II. Scheme C—Two Parallel Skewed Supports and One Radial Support

Girder 1 (Outside)

Location	Primary Moment, k-ft (1)	MSC/NASTRAN Moment, k-ft (2)	V-Load-Analysis Moment, k-ft (3)	Percentage Error $100 \frac{(3)-(2)}{(2)}$
Positive moment in Span 1 (0.44L ₁)	+2597.1 (0.4L ₁)	+3326.2 (0.4L ₁)	+3378.6 (0.4L ₁)	+1.6
Negative moment—pier	-1254.7 (0.4L ₂)	-1653.1 (0.4L ₁)	-1317.6 (0.4L ₂)	-20.3
Positive moment in Span 2 (0.41L ₂)	-2233.4 (0.6L ₂)	+2468.8 (0.6L ₂)	+2566.9 (0.6L ₂)	+4.0

Girder 2

Location	Primary Moment, k-ft (1)	MSC/NASTRAN Moment, k-ft (2)	V-Load-Analysis Moment, k-ft (3)	Percentage Error $100 \frac{(3)-(2)}{(2)}$
Positive moment in Span 1 (0.44L ₁)	+2933.4 (0.4L ₁)	+2382.3 (0.4L ₁)	+3223.4 (0.4L ₁)	+35.3
Negative moment—pier	-1297.7 (0.6L ₁)	-1114.4 (0.6L ₂)	-1380.2 (0.6L ₁)	+23.9
Positive moment in Span 2 (0.44L ₂)	+2346.0 (0.6L ₂)	+1911.4 (0.6L ₂)	+2490.5 (0.6L ₂)	+30.3

Girder 3

Location	Primary Moment, k-ft (1)	MSC/NASTRAN Moment, k-ft (2)	V-Load-Analysis Moment, k-ft (3)	Percentage Error $100 \frac{(3)-(2)}{(2)}$
Positive moment in Span 1 (0.42L ₁)	+2949.1 (0.4L ₁)	+1944.1 (0.4L ₁)	+2701.8 (0.4L ₁)	+39.0
Negative moment—pier	-1348.7 (0.6L ₁)	-815.1 (0.6L ₁)	-1258.5 (0.6L ₁)	+54.4
Positive moment in Span 2 (0.53L ₂)	+2138.0 (0.6L ₂)	+1452.6 (0.6L ₂)	+2049.9 (0.6L ₂)	+41.1

Girder 4 (Inside)

Location	Primary Moment, k-ft (1)	MSC/NASTRAN Moment, k-ft (2)	V-Load-Analysis Moment, k-ft (3)	Percentage Error $100 \frac{(3)-(2)}{(2)}$
Positive moment in Span 1 (0.44L ₁)	+2617.0 (0.4L ₁)	+1991.5 (0.4L ₁)	+1875.4 (0.4L ₁)	-5.8
Negative moment—pier	-1221.3 (0.6L ₁)	-846.5 (0.6L ₁)	-941.3 (0.6L ₁)	+11.2
Positive moment in Span 2 (0.57L ₂)	+1726.0 (0.6L ₂)	+1613.9 (0.6L ₂)	+1494.5 (0.6L ₂)	-7.4

Table VI

Comparison of V-Load-Analysis Results with MSC/NASTRAN Results

$$\text{Combined Loads} = 1.3 \left[D + \frac{5}{3} (L + 1) \right]$$

D = DL1 + DL2
 L = AASHTO HS20 Truck
 Wheel Load
 I = AASHTO Impact Factor

I. Scheme A—Radial Supports

Girder 1 (Outside)	MSC/NASTRAN Moment, k-ft (1)	V-Load-Analysis Moment, k-ft (2)	Percentage Error 100 $\frac{(2)-(1)}{(1)}$
<u>Location</u>			
Positive moment in Span 1 (Live load—0.35L ₁)	+6741.0	+6722.8	−0.3
Negative moment—pier (Live load—0.35L ₁)	−5180.8	−4975.5	−4.0
Positive moment in Span 2 (Live load—0.55L ₂)	+3242.1	+3103.6	−4.3
Girder 2	MSC/NASTRAN Moment, k-ft (1)	V-Load-Analysis Moment, k-ft (2)	Percentage Error 100 $\frac{(2)-(1)}{(1)}$
<u>Location</u>			
Positive moment in Span 1 (Live load—0.35L ₁)	+4743.6	+5726.3	+20.7
Negative moment—pier (Live load—0.54L ₁)	−4424.4	−4604.5	+4.1
Positive moment in Span 2 (Live load—0.55L ₂)	+2504.1	+3120.6	+24.6
Girder 3	MSC/NASTRAN Moment, k-ft (1)	V-Load-Analysis Moment, k-ft (2)	Percentage Error 100 $\frac{(2)-(1)}{(1)}$
<u>Location</u>			
Positive moment in Span 1 (Live load—0.35L ₁)	+3639.7	+4383.5	+20.4
Negative moment—pier (Live load—0.54L ₁)	−3703.7	−3949.6	+6.6
Positive moment in Span 2 (Live load—0.55L ₂)	+2305.7	+2870.1	+24.5
Girder 4 (Inside)	MSC/NASTRAN Moment, k-ft (1)	V-Load-Analysis Moment, k-ft (2)	Percentage Error 100 $\frac{(2)-(1)}{(1)}$
<u>Location</u>			
Positive moment in Span 1 (Live load—0.35L ₁)	+3012.6	+2810.1	−6.7
Negative moment—pier (Live load—0.54L ₁)	−3128.5	−3018.7	−3.5
Positive moment in Span 2 (Live load—0.55L ₂)	+2503.3	+2433.9	−2.8

II. Scheme C—Two Parallel Skewed Supports and One Radial Support

Girder 1 (Outside)			
Location	MSC/NASTRAN Moment, k-ft (1)	V-Load-Analysis Moment, k-ft (2)	Percentage Error $100 \frac{(2)-(1)}{(1)}$
Positive moment in Span 1 (Live load— $0.4L_1$)	+5813.9	+5886.8	+1.3
Negative moment—pier (Live load— $0.4L_1$ — MSC/NASTRAN) (Live load— $0.4L_2$ — V-Load)	-5259.3	-4958.4	-5.7
Positive moment in Span 2 (Live load— $0.6L_2$)	+3580.9	+3709.7	+3.6
Girder 2			
Location	MSC/NASTRAN Moment, k-ft (1)	V-Load-Analysis Moment, k-ft (2)	Percentage Error $100 \frac{(2)-(1)}{(1)}$
Positive moment in Span 1 (Live load— $0.4L_1$)	+4546.6	+5366.8	+18.0
Negative moment—pier (Live load— $0.6L_2$ — MSC/NASTRAN) (Live load— $0.6L_1$ — V-Load)	-4378.1	-4557.3	+4.1
Positive moment in Span 2 (Live load— $0.6L_2$)	+2892.3	+3474.0	+20.1
Girder 3			
Location	MSC/NASTRAN Moment, k-ft (1)	V-Load-Analysis Moment, k-ft (2)	Percentage Error $100 \frac{(2)-(1)}{(1)}$
Positive moment in Span 1 (Live load— $0.4L_1$)	+3725.1	+4459.7	+19.7
Negative moment—pier (Live load— $0.6L_1$)	-3630.4	-3981.0	+9.7
Positive moment in Span 2 (Live load— $0.6L_2$)	+2217.6	+2828.1	+27.5
Girder 4 (Inside)			
Location	MSC/NASTRAN Moment, k-ft (1)	V-Load-Analysis Moment, k-ft (2)	Percentage Error $100 \frac{(2)-(1)}{(1)}$
Positive moment in Span 1 (Live load— $0.4L_1$)	+3340.3	+3293.8	-1.4
Negative moment—pier (Live load— $0.6L_1$)	-2977.1	-3226.9	+8.4
Positive moment in Span 2 (Live load— $0.6L_2$)	+2198.2	+2056.6	-6.4

Table VII
Curved Bridge with Lateral Bracing—Closed Framed

Scheme A—Radial Supports
Bracing = WT6X32.5 (A = 9.54 inch²)

I. Noncomposite—DL1

Girder 1 (Outside)

Location	MSC/NASTRAN Moment No Bracing, k-ft	MSC/NASTRAN Moment Bracing in Every Other Bay (Outside Bays), k-ft	MSC/NASTRAN Moment Bracing in All Bays, k-ft
Maximum moment in Span 1 (0.37L ₁)	+1731.6	+1340.6	+1315.9
Minimum moment— pier	-2157.9	-2017.1	-1963.9
Maximum moment in Span 2 (0.75L ₂)	+374.1	+345.3	+333.1

Girder 2

Location	MSC/NASTRAN Moment No Bracing, k-ft	MSC/NASTRAN Moment Bracing in Every Other Bay (Outside Bays), k-ft	MSC/NASTRAN Moment Bracing in All Bays, k-ft
Maximum moment in Span 1 (0.37L ₁)	+1347.9	+1224.0	+1184.4
Minimum moment— pier	-1947.4	-1929.8	-1894.2
Maximum moment in Span 2 (0.75L ₂)	+382.8	+365.7	+333.8

Girder 3

Location	MSC/NASTRAN Moment No Bracing, k-ft	MSC/NASTRAN Moment Bracing in Every Other Bay (Outside Bays), k-ft	MSC/NASTRAN Moment Bracing in All Bays, k-ft
Maximum moment in Span 1 (0.37L ₁)	+984.1	+964.6	+915.3
Minimum moment— pier	-1692.9	-1666.0	-1619.1
Maximum moment in Span 2 (0.67L ₂)	+425.4	+376.0	+355.4

Girder 4 (Inside)

Location	MSC/NASTRAN Moment No Bracing, k-ft	MSC/NASTRAN Moment Bracing in Every Other Bay (Outside Bays), k-ft	MSC/NASTRAN Moment Bracing in All Bays, k-ft
Maximum moment in Span 1 (0.37L ₁)	+625.0	+652.8	+632.8
Minimum moment— pier	-1313.7	-1264.6	-1226.3
Maximum moment in Span 2 (0.67L ₂)	+461.9	+401.0	+371.7

II. Composite—DL2

Girder 1 (Outside)

Location	MSC/NASTRAN Moment No Bracing, k-ft	MSC/NASTRAN Moment Bracing in Every Other Bay (Outside Bays), k-ft	MSC/NASTRAN Moment Bracing in All Bays, k-ft
Maximum moment in Span 1 (0.42L ₁)	+647.7	+513.0	+490.0
Minimum moment— pier	−653.9	−573.8	−551.5
Maximum moment in Span 2 (0.68L ₂)	+164.8	+177.1	+169.2

Girder 2

Location	MSC/NASTRAN Moment No Bracing, k-ft	MSC/NASTRAN Moment Bracing in Every Other Bay (Outside Bays), k-ft	MSC/NASTRAN Moment Bracing in All Bays, k-ft
Maximum moment in Span 1 (0.42L ₁)	+499.3	+480.1	+440.7
Minimum moment— pier	−567.1	−546.6	−512.1
Maximum moment in Span 2 (0.68L ₂)	+168.5	+168.8	+153.4

Girder 3

Location	MSC/NASTRAN Moment No Bracing, k-ft	MSC/NASTRAN Moment Bracing in Every Other Bay (Outside Bays), k-ft	MSC/NASTRAN Moment Bracing in All Bays, k-ft
Maximum moment in Span 1 (0.42L ₁)	+357.8	+392.9	+379.1
Minimum moment— pier	−482.8	−467.2	−464.1
Maximum moment in Span 2 (0.68L ₂)	+172.8	+155.2	+150.7

Girder 4 (Inside)

Location	MSC/NASTRAN Moment No Bracing, k-ft	MSC/NASTRAN Moment Bracing in Every Other Bay (Outside Bays), k-ft	MSC/NASTRAN Moment Bracing in All Bays, k-ft
Maximum moment in Span 1 (0.42L ₁)	+219.7	+308.7	+319.4
Minimum moment pier	−366.0	−383.4	−384.5
Maximum moment in Span 2 (0.67L ₂)	+170.9	+151.1	+144.1

III. Live Load—Two AASHTO HS20 Trucks

Girder 1 (Outside)

Location	MSC/NASTRAN Moment No Bracing, k-ft	MSC/NASTRAN Moment Bracing in Every Other Bay (Outside Bays), k-ft	MSC/NASTRAN Moment Bracing in All Bays, k-ft
Positive moment in Span 1 (0.42L ₁)	+3648.0 (0.35L ₁)	+2504.7 (0.35L ₁)	+2320.6 (0.35L ₁)
Negative moment—pier	-1525.4 (0.35L ₁)	-1186.3 (0.35L ₁)	-913.2 (0.35L ₁)
Positive moment in Span 2 (0.54L ₂)	+2541.6 (0.55L ₂)	+1768.2 (0.55L ₂)	+1615.6 (0.55L ₂)

Girder 2

Location	MSC/NASTRAN Moment No Bracing, k-ft	MSC/NASTRAN Moment Bracing in Every Other Bay (Outside Bays), k-ft	MSC/NASTRAN Moment Bracing in All Bays, k-ft
Positive moment in Span 1 (0.42L ₁)	+2342.2 (0.35L ₁)	+2175.7 (0.35L ₁)	+1977.4 (0.35L ₁)
Negative moment—pier	-1155.6 (0.54L ₁)	-1128.0 (0.54L ₁)	-959.3 (0.54L ₁)
Positive moment in Span 2 (0.53L ₂)	+1787.3 (0.55L ₂)	+1591.5 (0.55L ₂)	+1403.4 (0.55L ₂)

Girder 3

Location	MSC/NASTRAN Moment No Bracing, k-ft	MSC/NASTRAN Moment Bracing in Every Other Bay (Outside Bays), k-ft	MSC/NASTRAN Moment Bracing in All Bays, k-ft
Positive moment in Span 1 (0.37L ₁)	+1895.2 (0.35L ₁)	+1834.1 (0.35L ₁)	+1822.0 (0.35L ₁)
Negative moment—pier	-875.3 (0.54L ₁)	-817.2 (0.54L ₁)	-818.3 (0.54L ₁)
Positive moment in Span 2 (0.53L ₂)	+1528.2 (0.55L ₂)	+1401.5 (0.55L ₂)	+1262.4 (0.55L ₂)

Girder 4 (Inside)

Location	MSC/NASTRAN Moment No Bracing, k-ft	MSC/NASTRAN Moment Bracing in Every Other Bay (Outside Bays), k-ft	MSC/NASTRAN Moment Bracing in All Bays, k-ft
Positive moment in Span 1 (0.37L ₁)	+1914.5 (0.35L ₁)	+1553.1 (0.35L ₁)	+1579.5 (0.35L ₁)
Negative moment—pier	-944.9 (0.54L ₁)	-809.0 (0.54L ₁)	-746.7 (0.54L ₁)
Positive moment in Span 2 (0.53L ₂)	+1680.7 (0.55L ₂)	+1331.2 (0.55L ₂)	+1321.7 (0.55L ₂)

Table VIII
St. Venant Torsion vs. Warping Torsion

Scheme A—Radial Supports Noncomposite—DL1

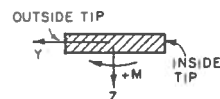
Girder 1 (Outside)

Location	St. Venant Torque, T_{sv} , k-ft	Warping Torque, T_w , k-ft
0.11L ₁	-0.35	-8.31
0.26L ₁	-0.09	+15.75
0.42L ₁	-0.13	-17.62
0.57L ₁	+0.20	+13.65
0.73L ₁	+0.18	-3.87
0.88L ₁	+0.30	-9.36
0.98L ₁	+0.26	-16.76
	—Pier—	
0.18L ₂	+0.31	+13.27
0.39L ₂	-0.01	-2.74
0.61L ₂	-0.15	-1.72
0.82L ₂	-0.01	+1.79
0.96L ₂	-0.02	+0.49

Table IX
Flange Warping and Bending Moments, and Warping Stresses

Scheme A—Radial Supports Girder 1 (Outside)

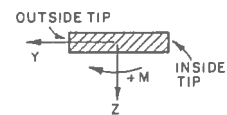
I. Noncomposite—DL1



Cross Frame No.	Warping Moment MSC/NASTRAN,* M_{fw} , k-ft (1)		Warping Moment Straight— Flange Model, M_{fw} , k-ft (2)		Additional Lateral Bending Moment MSC/NASTRAN,* M_{fb} , k-ft (3)	
	Top Flange	Bottom Flange	Top Flange	Bottom Flange	Top Flange	Bottom Flange
2	+3.17	-3.17	+3.65	-3.65	+0.26	+0.58
3	+7.05	-7.05	+7.77	-7.77	+0.28	+0.63
4	+9.02	-9.02	+9.98	-9.98	+0.30	+0.68
5	+9.67	-9.67	+10.79	-10.78	+0.31	+0.70
6	+8.88	-8.88	+9.97	-9.98	+0.28	+0.65
7	+6.71	-6.71	+7.67	-7.62	+0.23	+0.53
8	+3.17	-3.17	+3.80	-3.95	+0.12	+0.27
9	-1.41	+1.41	-0.80	+1.37	+0.19	+0.23
10	-5.78	+5.78	-6.10	+5.93	-0.50	-0.61
Pier—11	-9.92	+9.92	-10.28	+10.36	+0.49	+0.60
12	-9.65	+9.65	-10.58	+10.42	-0.45	-0.55
13	-3.46	+3.46	-3.64	+3.67	-0.017	-0.024
14	-0.38	+0.38	-0.64	+0.63	-0.057	-0.078
15	+1.28	-1.28	+1.13	-1.13	+0.002	+0.003
16	+1.30	-1.30	+1.17	-1.17	-0.04	-0.054
17	+1.06	-1.06	+0.98	-0.98	-0.074	-0.102

*From the curved-bridge model.

Table IX (Continued)



Cross Frame No.	Warping Moment Refined Straight—Flange Model, M_{fw} , k-ft (4)		Approximate Warping Moment $\frac{Md^2}{12hR}$, M_{fw} , k-ft (5)		Warping Normal Stress, $\pm\sigma_w$, ksi (6)	
	Top Flange	Bottom Flange	Top Flange	Bottom Flange	Top Flange	Bottom Flange
2	+4.52	-4.52	+4.31	-4.31	1.76	0.78
3	+9.78	-9.78	+10.22	-10.22	4.18	1.84
4	+12.53	-12.53	+13.31	-13.31	5.44	2.40
5	+13.54	-13.54	+14.34	-14.34	<u>5.87</u>	<u>2.58</u>
6	+12.51	-12.53	+13.27	-13.27	5.43	2.39
7	+9.61	-9.57	+10.16	-10.16	4.16	1.83
8	+4.79	-4.95	+5.14	-5.14	2.10	0.93
9	-0.97	+1.57	-1.49	+1.49	0.61	0.27
10	-7.23	+7.05	-8.39	+8.39	1.72	1.40
Pier—11	-12.58	+12.66	-14.78	+14.78	3.02	2.46
12	-12.35	+12.20	-11.69	+11.69	2.39	1.95
13	-4.56	+4.59	-5.59	+5.59	3.14	2.29
14	-0.66	+0.65	-0.82	+0.82	0.46	0.34
15	+1.49	-1.48	+1.09	-1.09	0.61	0.45
16	+1.48	-1.48	+1.65	-1.65	0.93	0.67
17	+1.27	-1.27	+1.27	-1.27	0.71	0.52

III. Live load—Two AASHTO HS20 Trucks

II. Composite—DL2

II. Composite—DL2			Load at 0.35L ₁		Load at 0.55L ₂		
Cross Frame No.	Approximate Warping Moment $\frac{Md^2}{12hR}$ M _{fw} , k-ft (7) <u>Bottom Flange</u>	Flange Warping Normal Stress $\pm\sigma_w$, ksi (8) <u>Bottom Flange</u>	Cross Frame No.	Approximate	Warping	Approximate	Warping
				Moment	Normal	Moment	Normal
				$\frac{Md^2}{12hR}$	Stress,	$\frac{Md^2}{12hR}$	Stress,
				M _{fw} , k-ft	$\pm\sigma_w$, ksi	M _{fw} , k-ft	$\pm\sigma_w$, ksi
				(9)	(10)	(11)	(12)
				Bottom Flange	Bottom Flange	Bottom Flange	Bottom Flange
2	-1.57	0.28	2	-6.56	1.18	+0.94	0.17
3	-3.75	0.68	3	-17.55	3.16	+2.53	0.46
4	-4.95	0.89	4	-25.78	4.64	+3.85	0.69
5	-5.44	<u>0.98</u>	5	-29.93	<u>5.39</u>	+5.07	0.91
6	-5.19	<u>0.93</u>	6	-27.91	5.02	+6.15	1.11
7	-4.23	0.76	7	-20.96	3.77	+7.04	1.27
8	-2.59	0.47	8	-13.02	2.34	+7.71	1.39
9	-0.36	0.06	9	-4.75	0.86	+8.21	1.48
10	+2.18	0.36	10	+3.27	0.55	+7.35	1.23
Pier—11	+4.45	0.74	Pier—11	+9.64	1.61	+6.77	1.13
12	+3.23	0.54	12	+11.22	1.87	-1.24	0.21
13	+1.15	0.47	13	+10.21	4.18	-11.37	4.65
14	-0.40	0.16	14	+8.40	3.44	-18.85	<u>7.71</u>
15	-0.63	0.26	15	+3.22	1.32	-9.87	4.04
16	-0.74	0.30	16	+2.18	0.89	-7.36	3.01
17	-0.52	0.21	17	+1.10	0.45	-3.77	1.54

Table X
Flange Warping Moments and Stresses

Scheme C—Two Parallel Skewed Supports and One Radial Support Girder 1 (Outside)

I. Noncomposite—DL1					II. Composite—DL2	
Cross Frame No.	Approximate Warping Moment $\frac{Md^2}{12hR}$ M_{fw} , k-ft (1)		Warping Normal Stress $\pm \sigma_w$, ksi (2)		Approximate Warping Moment $\frac{Md^2}{12hR}$, M_{fw} , k-ft (3)	Warping Normal Stress, $\pm \sigma_w$, ksi (4)
	Top Flange	Bottom Flange	Top Flange	Bottom Flange	Bottom Flange	Bottom Flange
2	+5.46	-5.46	2.46	1.29	-2.01	0.48
3	+9.27	-9.27	4.17	2.20	-3.45	0.82
4	+11.17	-11.17	5.03	2.65	-4.24	1.00
5	+11.04	-11.04	4.97	2.61	-4.33	1.03
6	+8.86	-8.86	3.99	2.10	-3.70	0.88
7	+4.70	-4.70	2.12	1.11	-2.37	0.56
8	-1.24	+1.24	0.56	0.29	-0.37	0.09
9	-8.73	+8.73	1.79	1.51	+2.22	0.38
10	-14.11	+14.11	2.80	2.44	+4.26	0.74
Across Pier—11	-10.75	+10.75	2.20	1.86	+3.01	0.52
12	-6.05	+6.05	1.24	1.05	+1.24	0.21
13	-0.72	+0.72	0.40	0.32	-0.57	0.26
14	+3.15	-3.15	1.77	1.42	-1.75	0.79
15	+2.59	-2.59	1.46	1.17	-1.14	0.51
16	+2.66	-2.66	1.50	1.20	-1.08	0.49
17	+1.78	-1.78	1.00	0.80	-0.69	0.31

III. Live Load—Two AASHTO HS20 Trucks

Cross Frame No.	Load at $0.4L_1$		Load at $0.6L_2$	
	Approximate Warping Moment $\frac{Md^2}{12hR}$ M_{fw} , k-ft (5)	Warping Normal Stress, $\pm \sigma_w$, ksi (6)	Approximate Warping Moment $\frac{Md^2}{12hR}$, M_{fw} , k-ft (7)	Warping Normal Stress, $\pm \sigma_w$, ksi (8)
	Bottom Flange	Bottom Flange	Bottom Flange	Bottom Flange
2	-8.76	2.07	+1.61	0.38
3	-17.25	4.09	+3.18	0.75
4	-24.43	5.79	+4.68	1.11
5	-27.62	6.54	+6.07	1.44
6	-24.70	5.85	+7.31	1.73
7	-16.90	4.00	+8.37	1.98
8	-8.22	1.95	+9.35	2.21
9	+1.11	0.19	+9.63	1.67
10	+8.38	1.45	+8.23	1.42
Across Pier—11	+9.36	1.62	+2.64	0.46
12	+10.50	1.82	-6.40	1.11
13	+9.13	4.11	-15.23	6.85
14	+7.65	3.44	-21.99	9.90
15	+2.94	1.32	-11.05	4.97
16	+1.99	0.90	-8.15	3.67
17	+1.00	0.45	-4.17	1.88

14. FIGURES

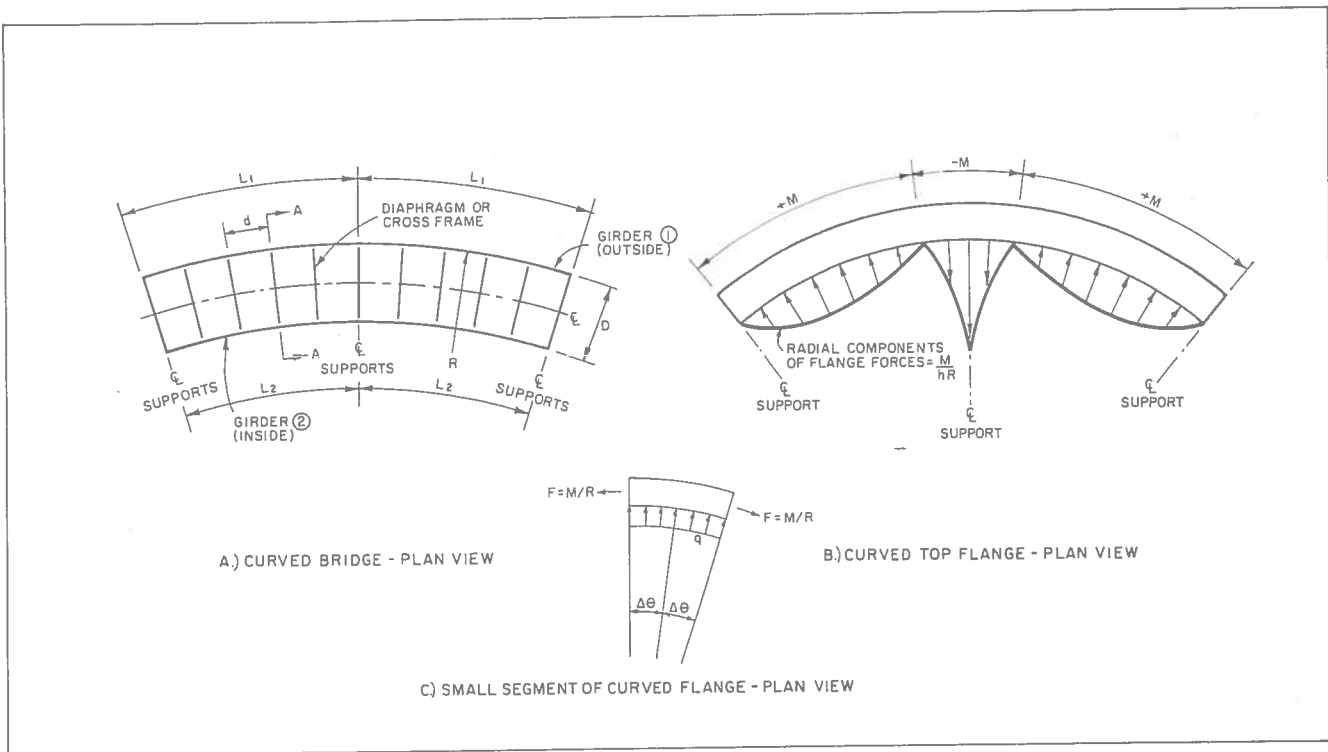


Figure 1. Development of lateral flange forces in curved bridges.

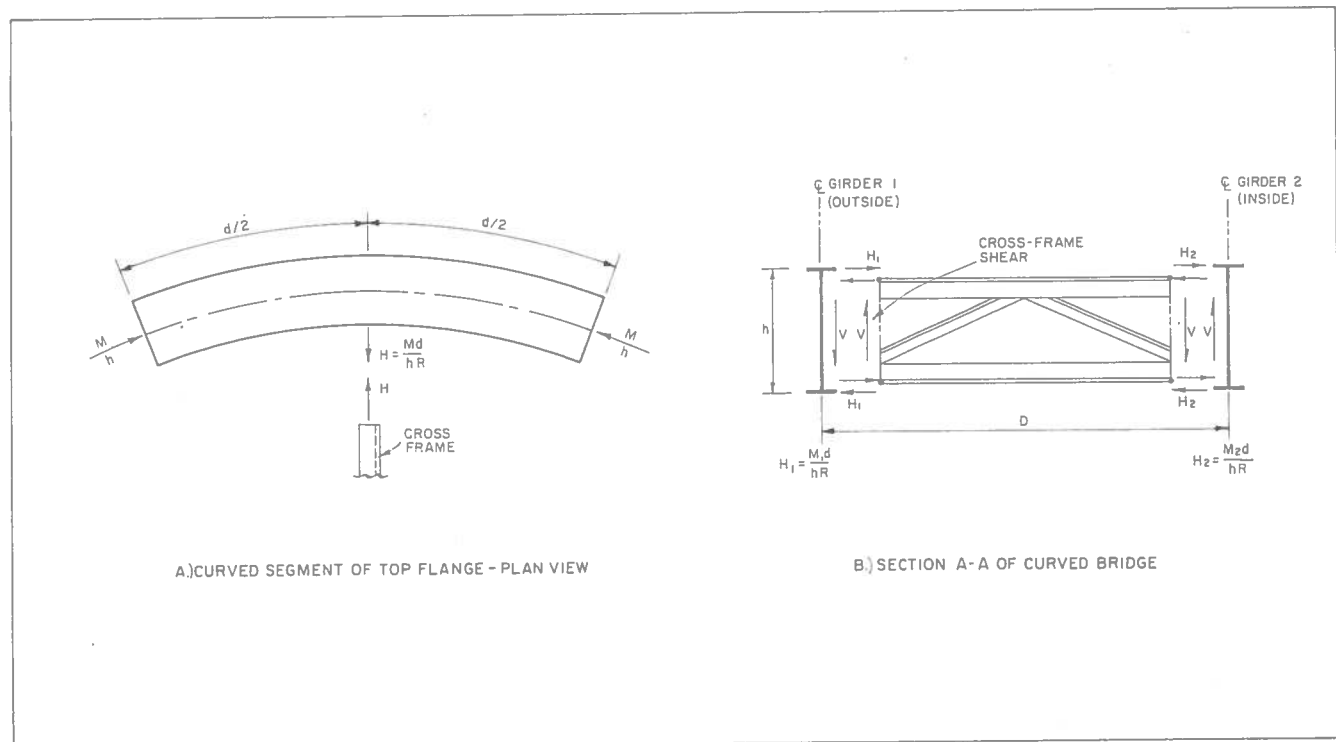


Figure 2. Cross-frame forces.

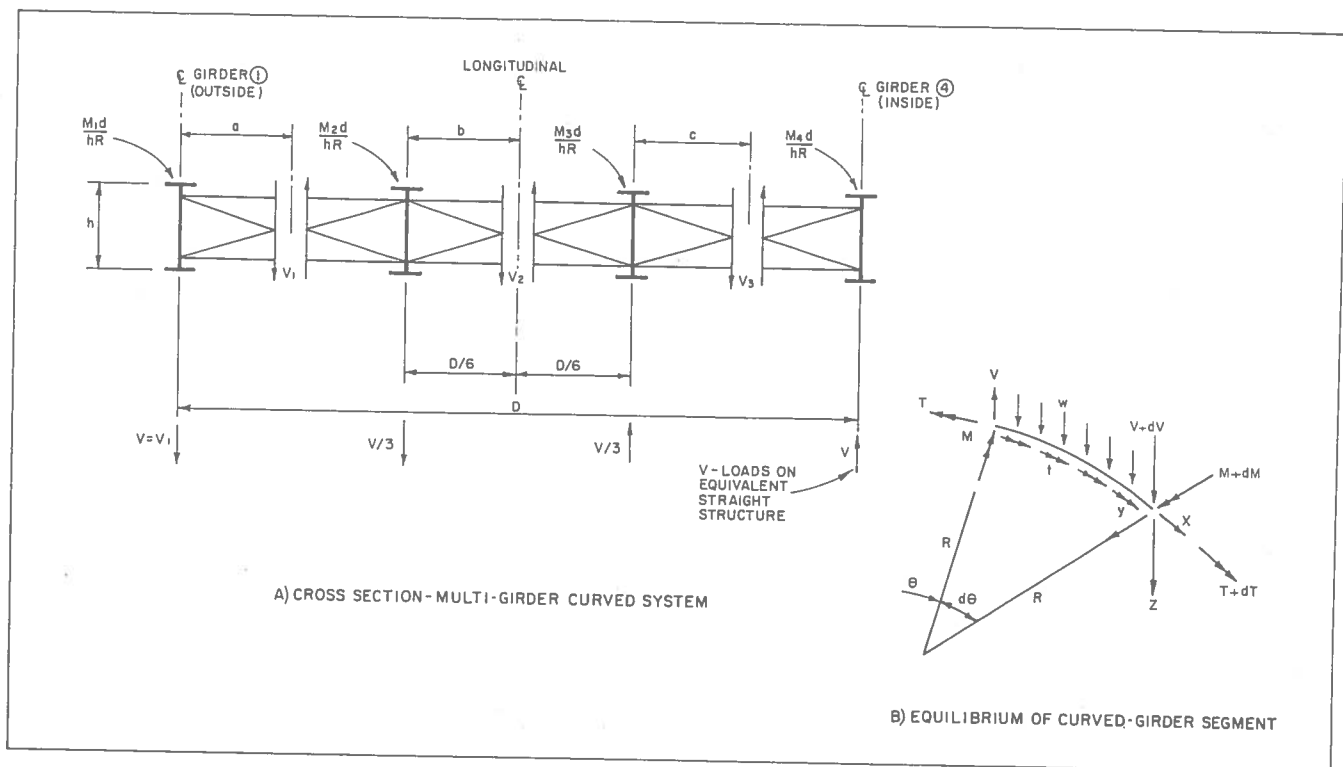


Figure 3. Curved girder forces.

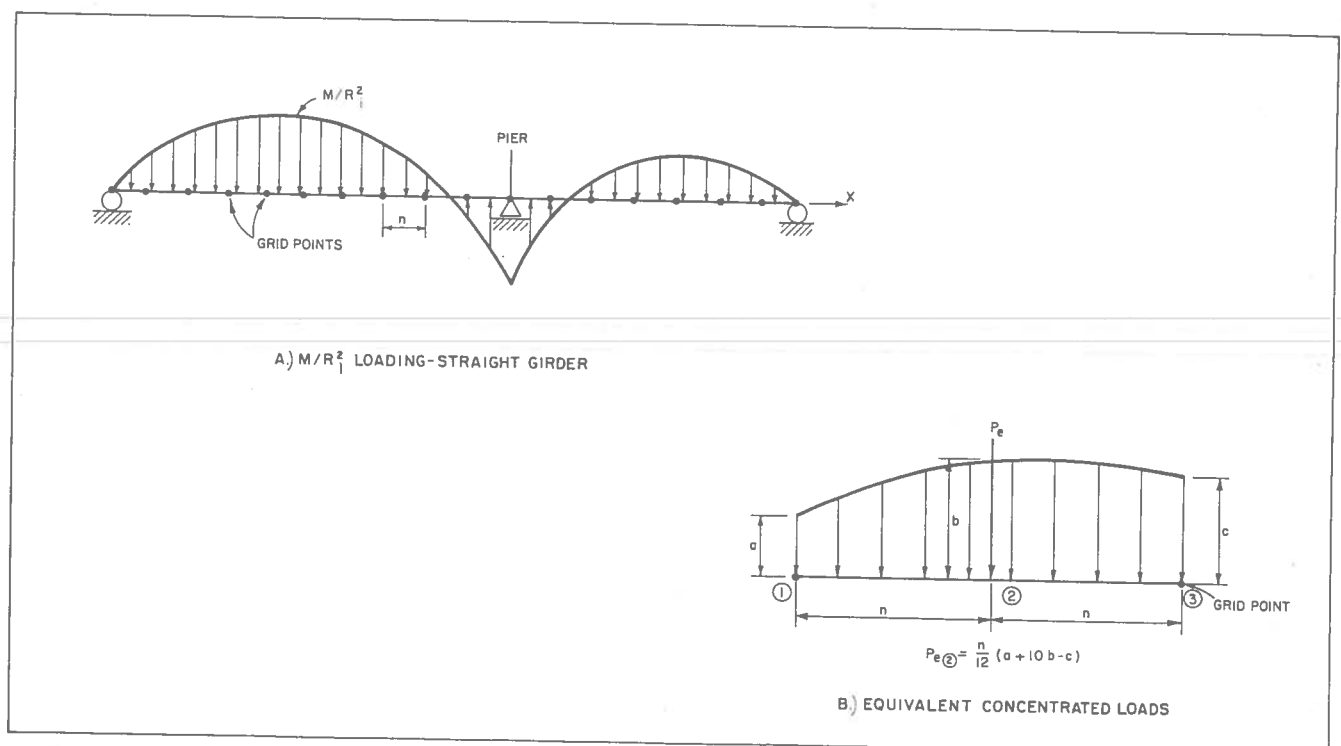


Figure 4. M/R_i^2 loads.

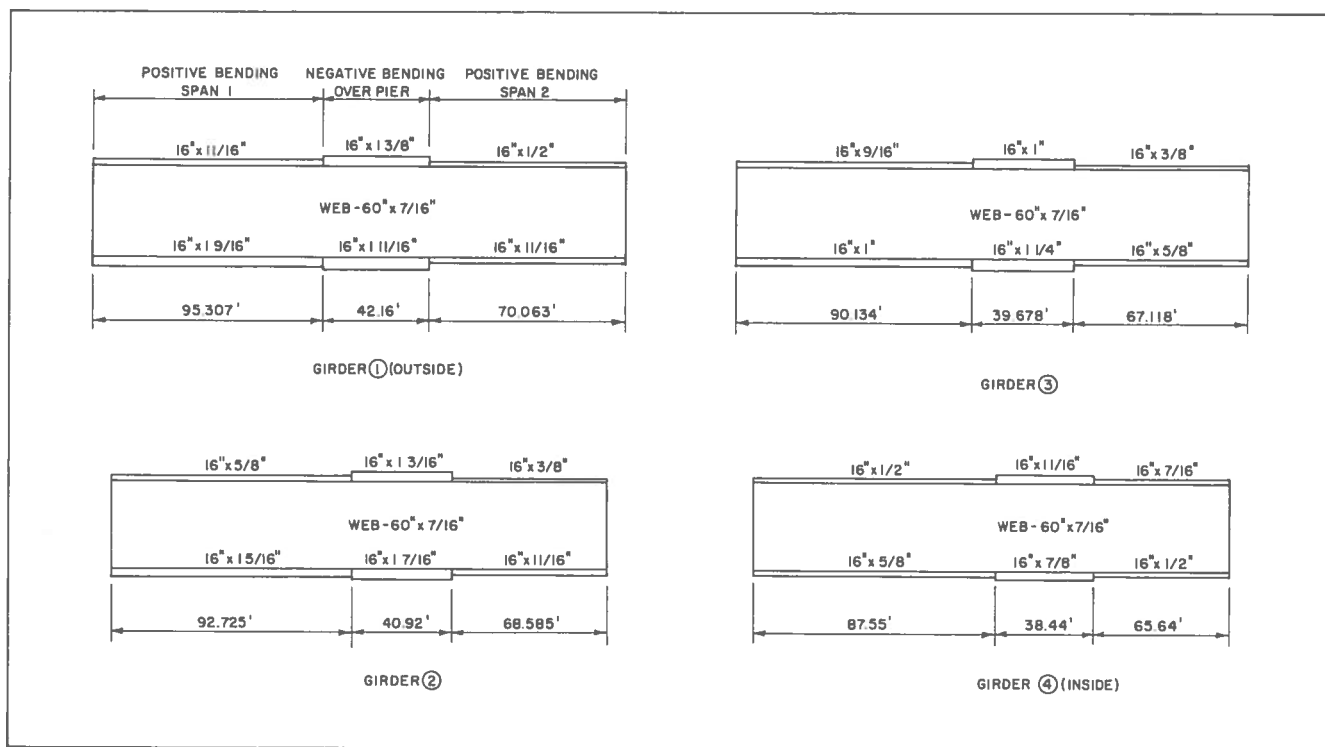


Figure 7. Elevations of typical girders; Scheme A.

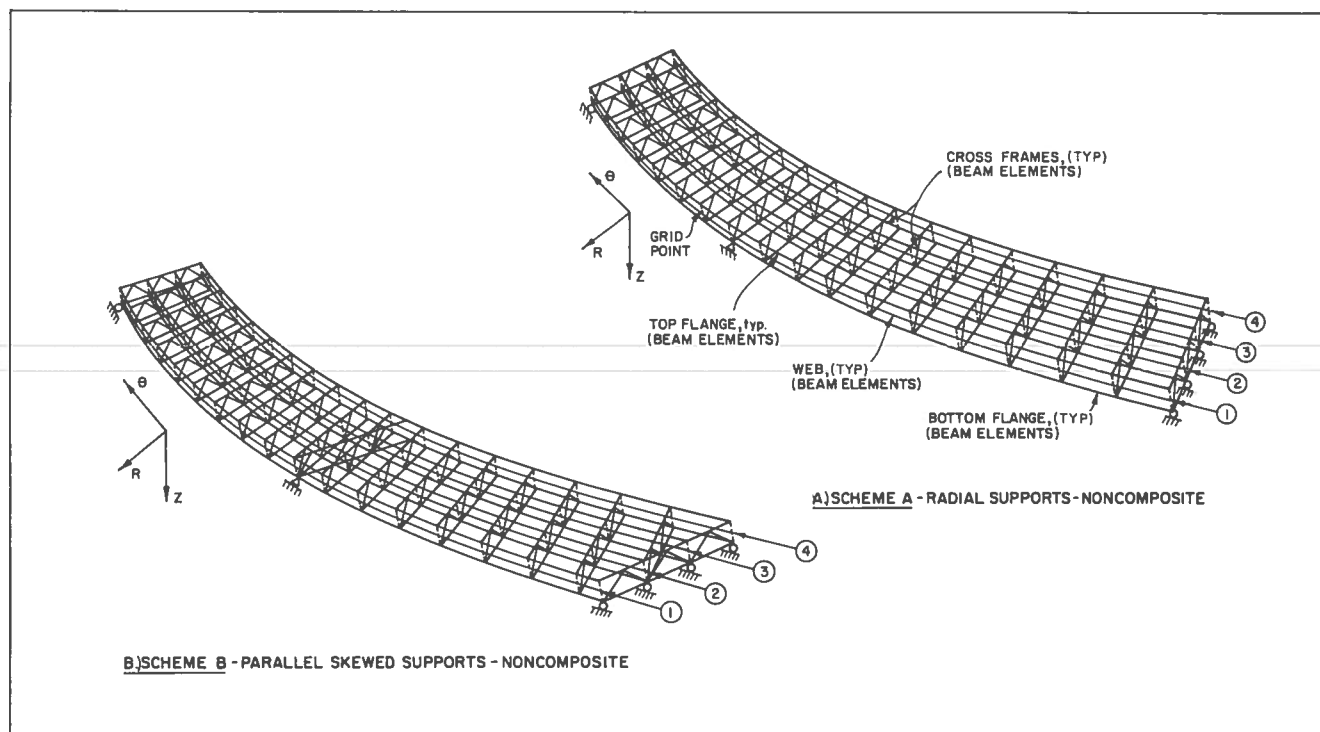


Figure 8. MSC/NASTRAN finite-element models: non-composite Schemes A and B.

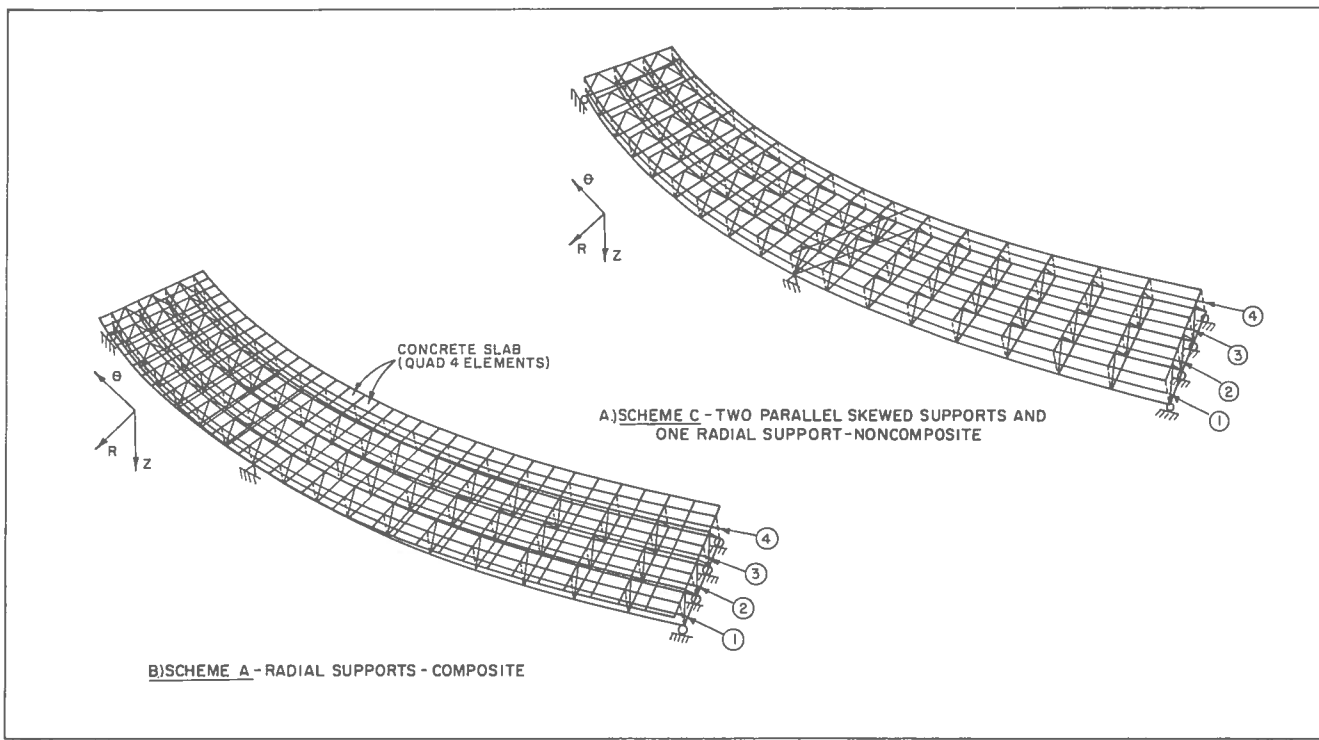


Figure 9. MSC/NASTRAN finite-element models: non-composite Scheme C, composite Scheme A.

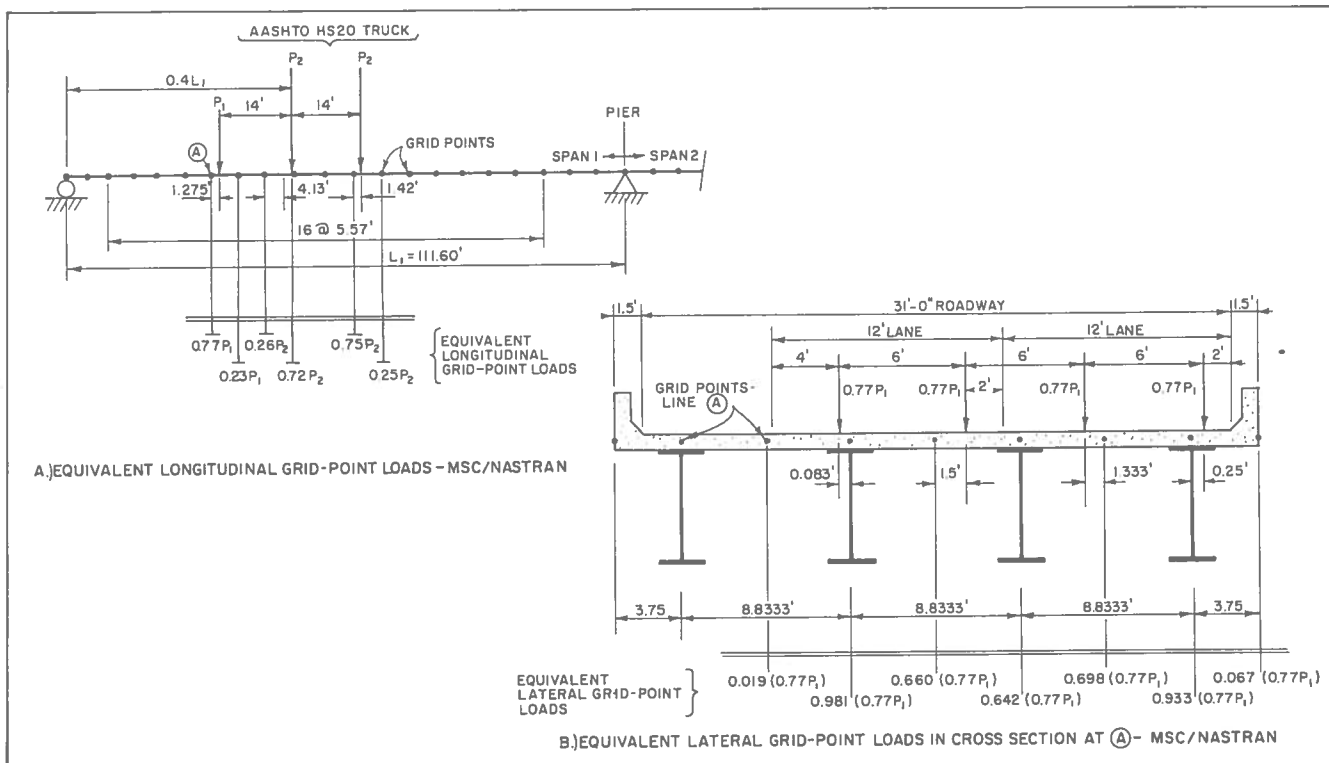


Figure 10. Equivalent grid-point loads for AASHTO HS20 trucks positioned to produce maximum moment in girder 4, Scheme C.

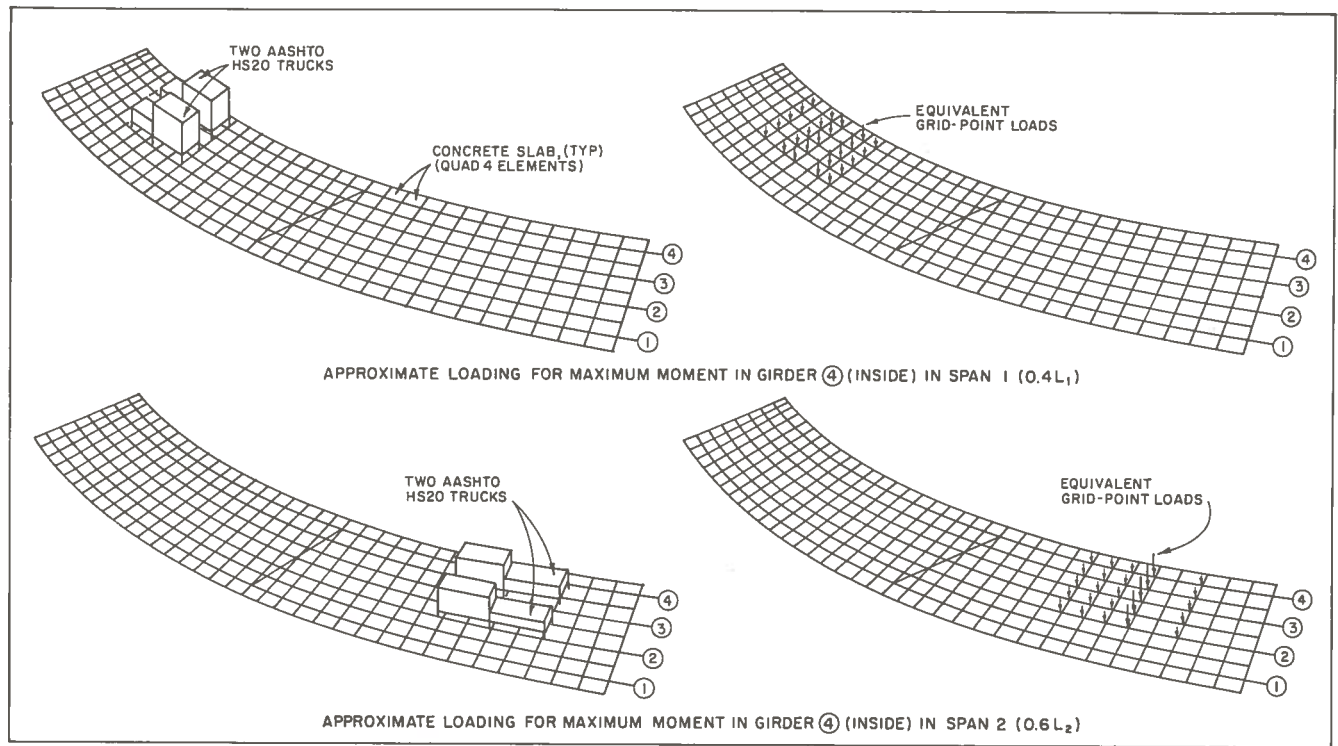


Figure 11. Live loads on MSC/NASTRAN finite-element model, Scheme C.

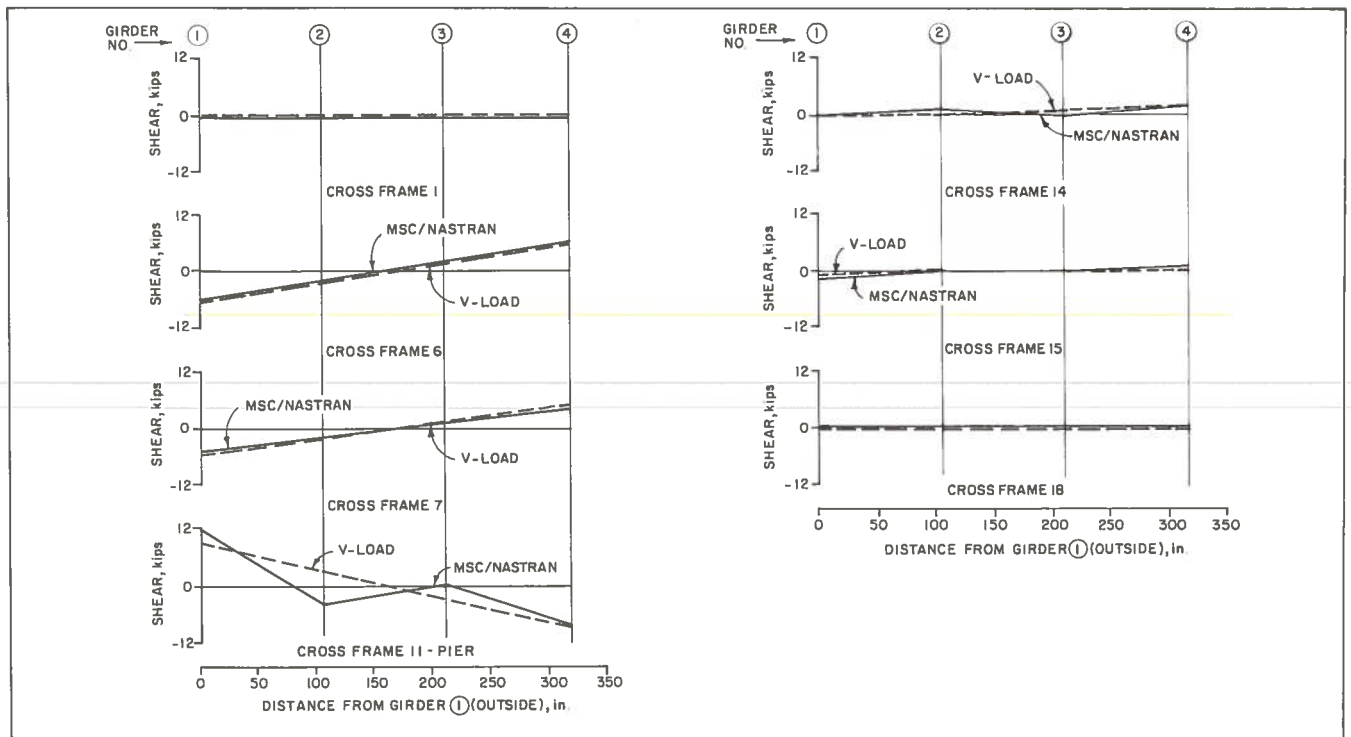
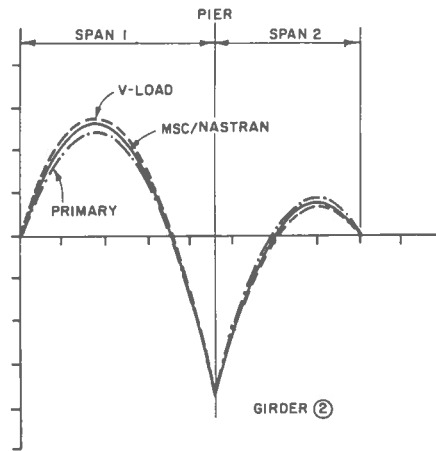
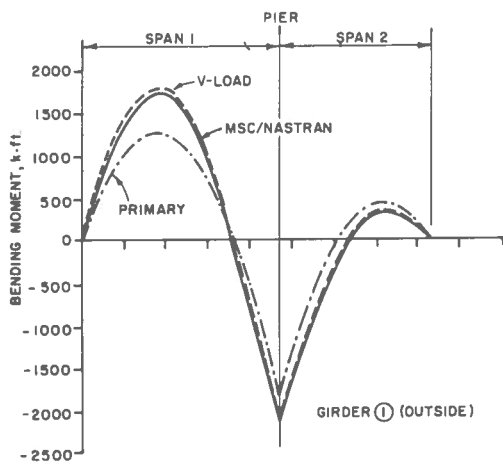


Figure 12. Comparison of shears: MSC/NASTRAN vs. V-Load method. Scheme A: radial supports, DL1 noncomposite.



- - - V-LOAD
 — MSC/NASTRAN
 - · - PRIMARY

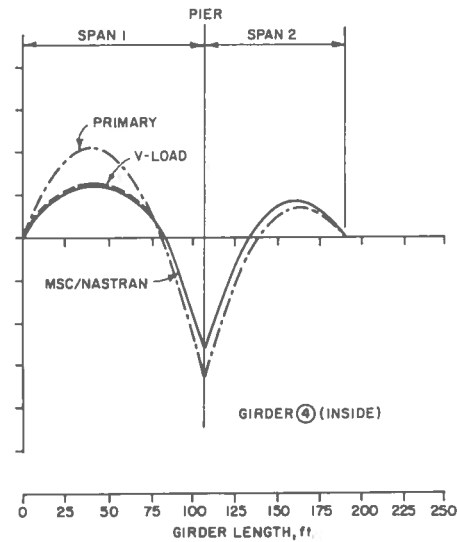
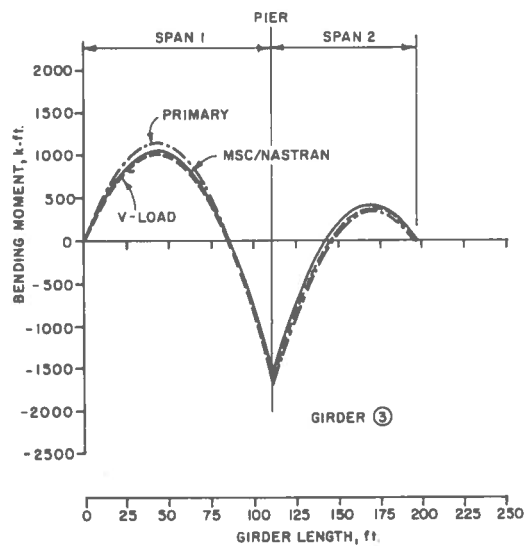


Figure 13. Comparison of moments: MSC/NASTRAN vs. V-Load method. Scheme A: radial supports, DL1 bending moments, noncomposite.

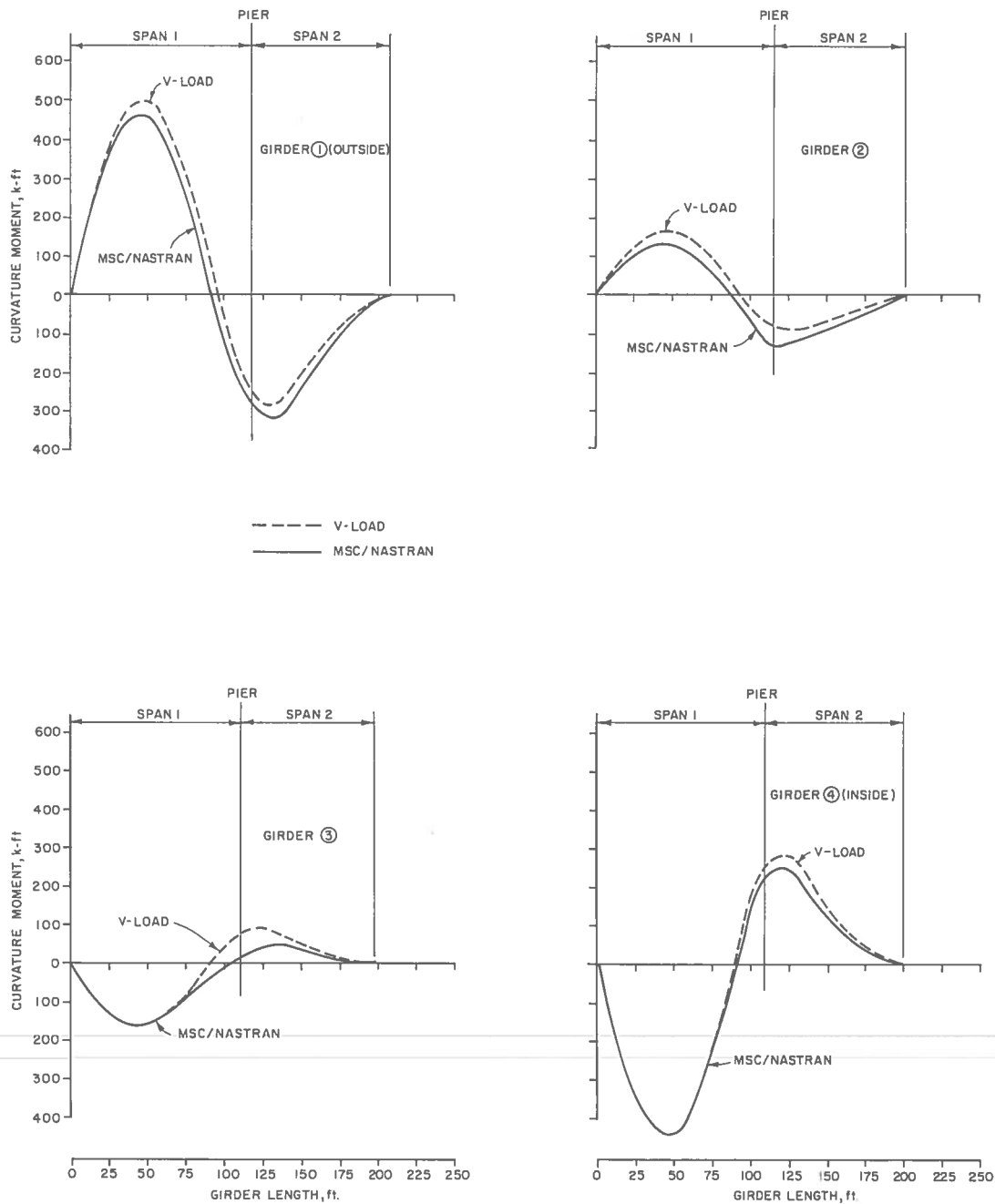
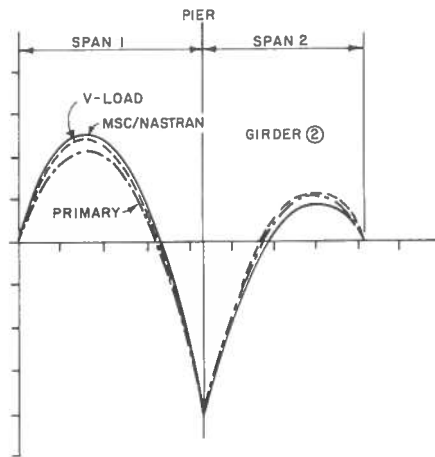
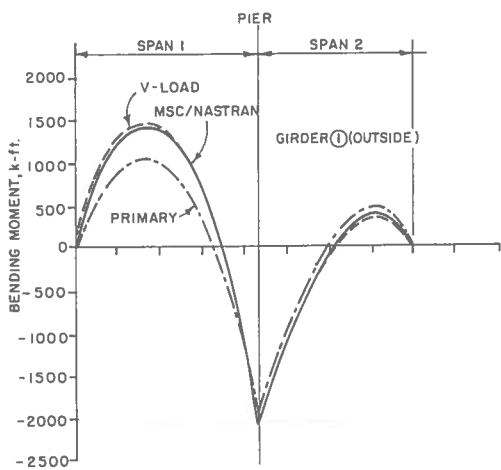


Figure 14. Comparison of moments: MSC/NASTRAN vs. V-Load method. Scheme A: radial supports, DL1 curvature moments, noncomposite.



- - - - V-LOAD
 ——— MSC/NASTRAN
 - · - · PRIMARY

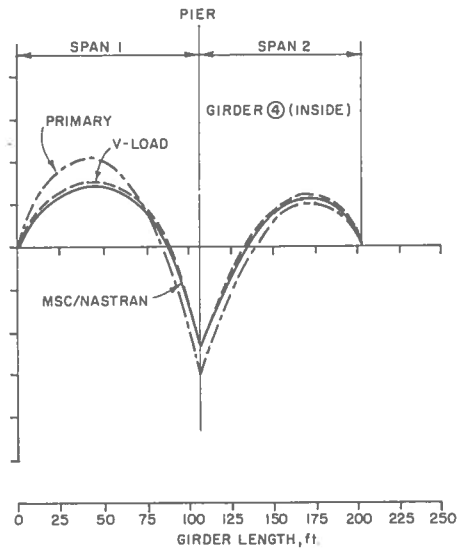
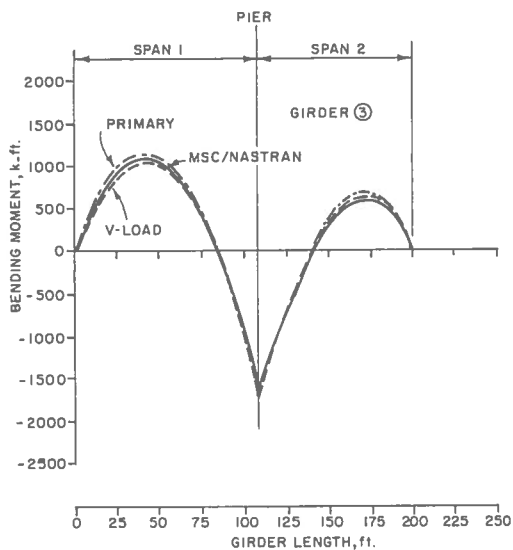


Figure 15. Comparison of moments: MSC/NASTRAN vs. V-Load method. Scheme B: parallel skewed supports, DL1 bending moments, noncomposite.

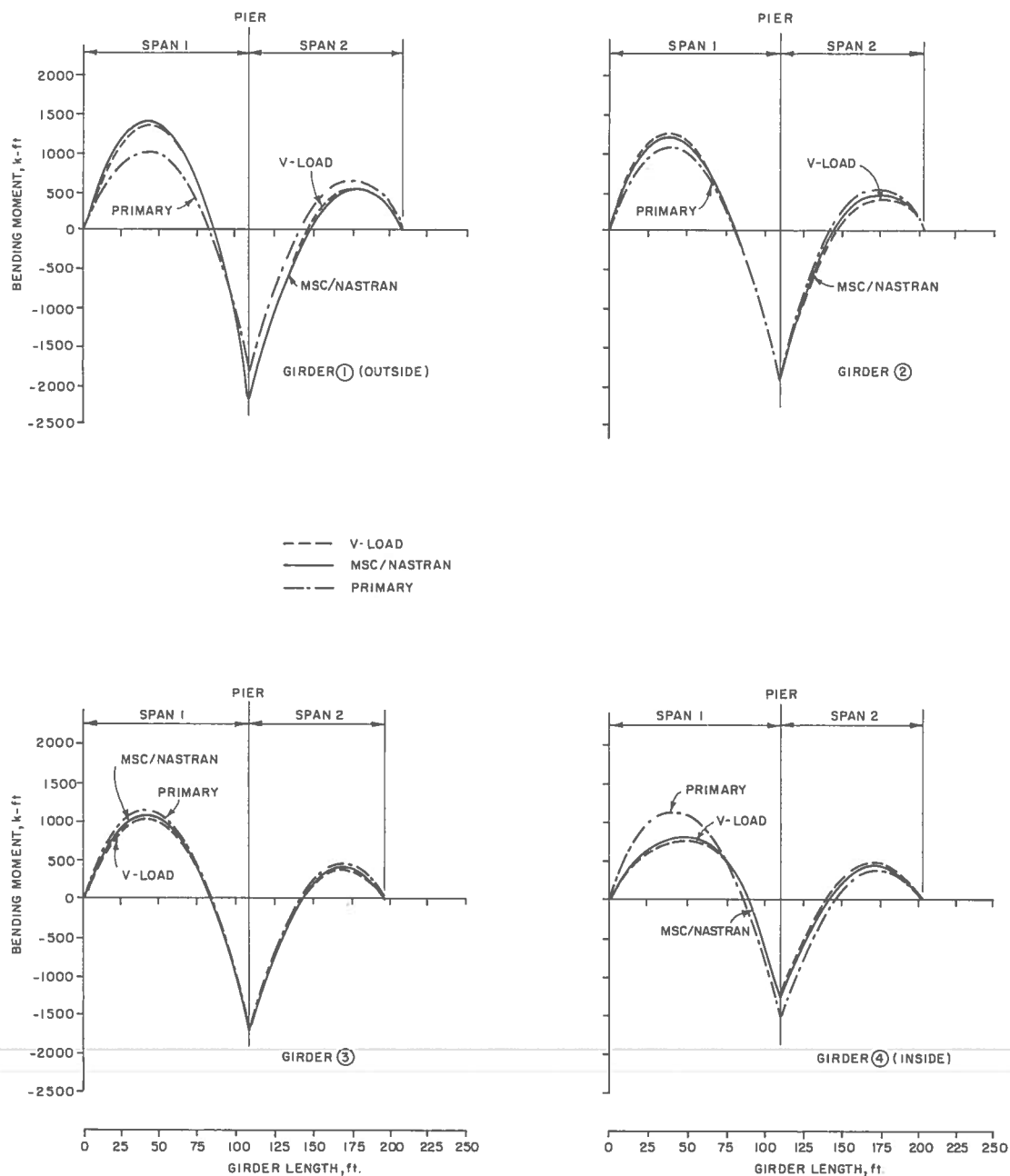


Figure 16. Comparison of moments: MSC/NASTRAN vs. V-Load method. Scheme C: two parallel skewed supports and one radial support, DL1 bending moments, noncomposite.

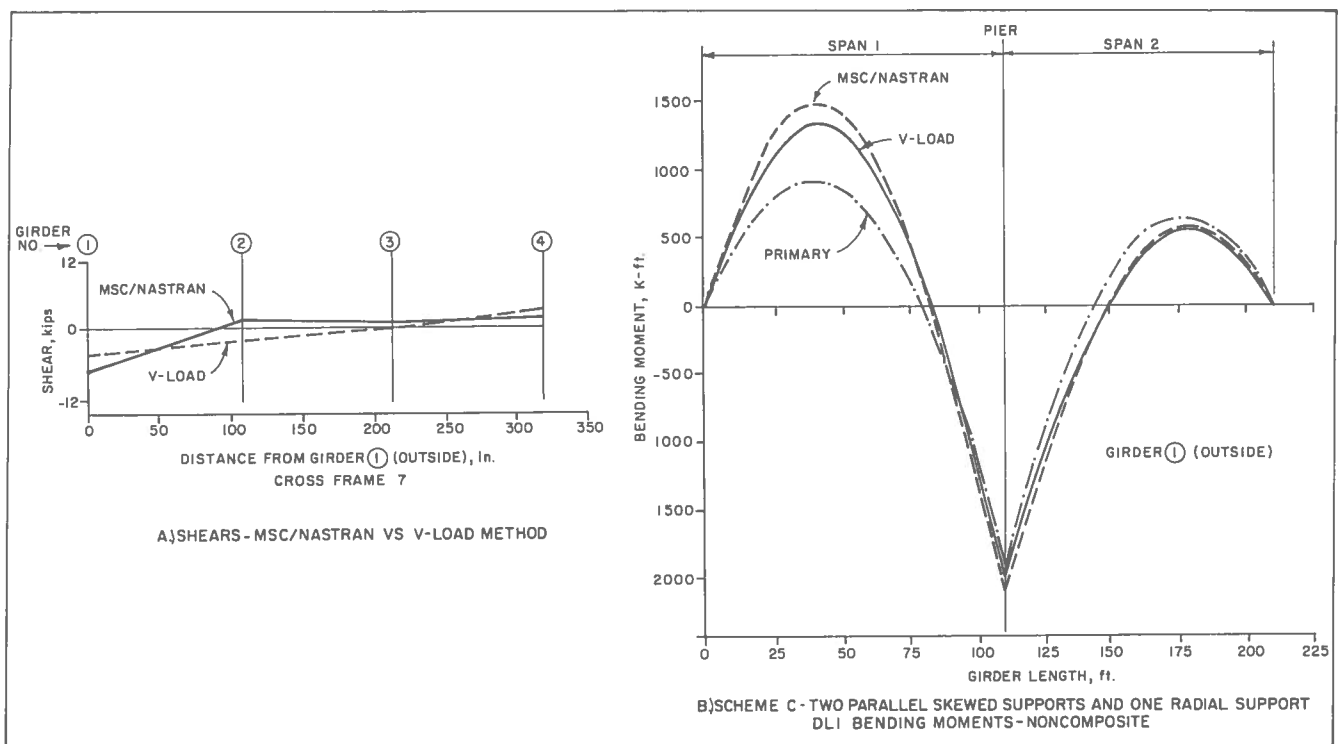


Figure 17. Comparison of MSC/NASTRAN vs. V-Load method. Dead-Load analysis results for girders having unequal stiffness.

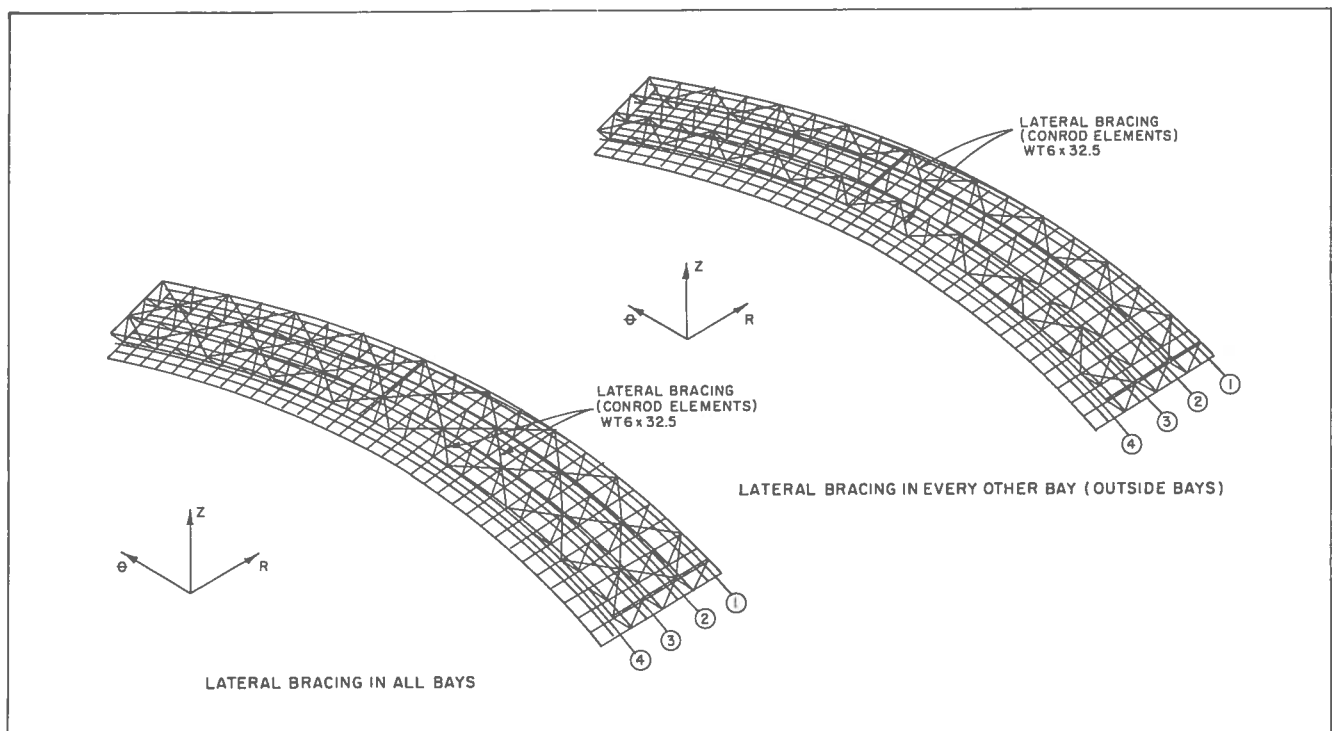


Figure 18. MSC/NASTRAN finite-element models with lateral bracing.

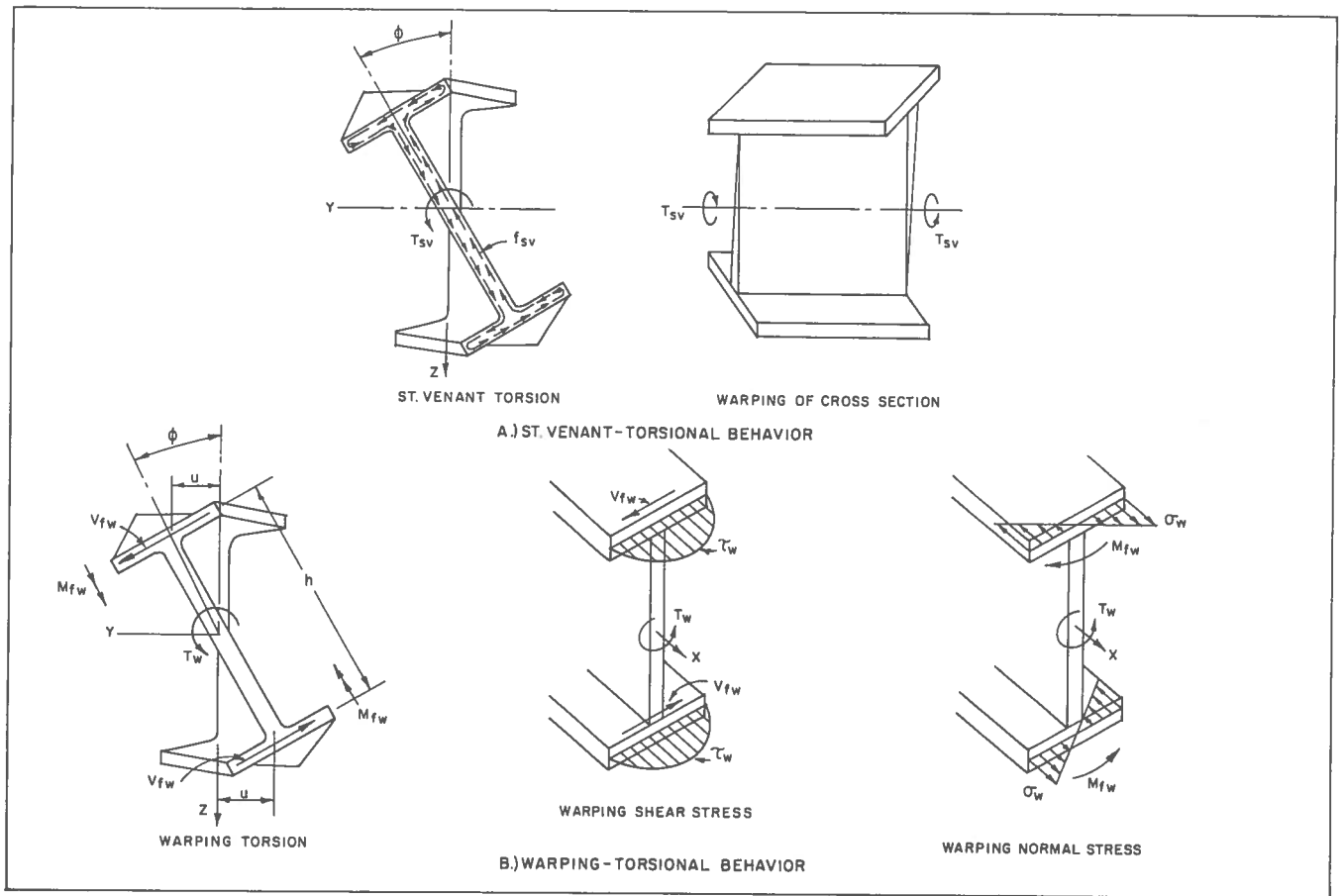


Figure 19. Stresses produced by torsion.

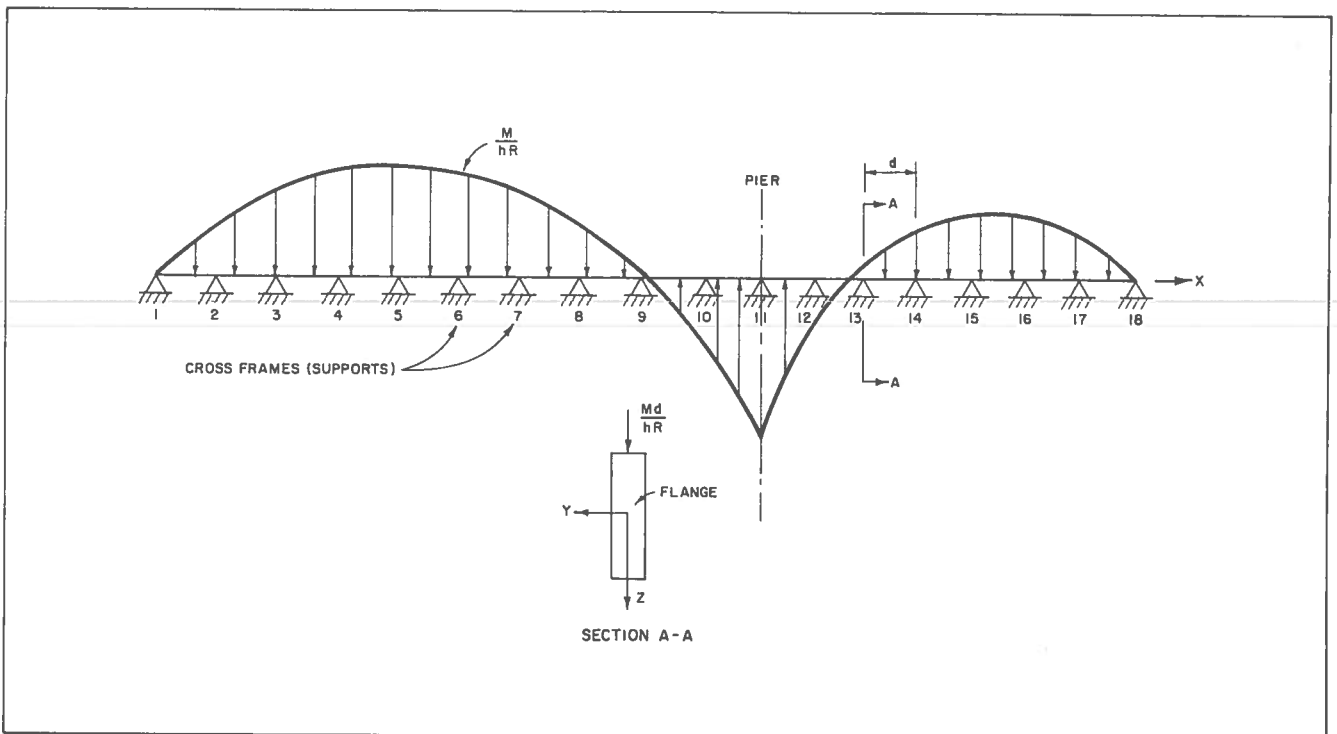


Figure 20. Equivalent lateral loads on the straight flange.

*For current technical information regarding products
of United States Steel Corporation, contact a USS
Construction Services Representative through your
nearest USS Sales Office or write:*

***United States Steel Corporation
P.O. Box 86
600 Grant Street
Pittsburgh, PA 15230***



United States Steel

600 Grant St., Pittsburgh, Pa. 15230

USS is a registered trademark
ADUSS 88-8535-01
Printed in U.S.A.
July 1984